Reliability Engineering and System Safety 229 (2023) 108845

Contents lists available at ScienceDirect

Reliability Engineering and System Safety

journal homepage: www.elsevier.com/locate/ress

The modeling of risk perception in the use of structural health monitoring information for optimal maintenance decisions

Mayank Chadha [a], Mukesh K. Ramancha [a], Manuel A. Vega [b], Joel P. Conte [a], Michael D. Todd [a,*]

[a] Department of Structural Engineering 0085, University of California San Diego, 9500 Gilman Drive, La Jolla, CA 92093-0085, United States of America
[b] Los Alamos National Laboratory, Los Alamos, NM 87545, United States of America

ARTICLE INFO

Keywords:
Expected utility theory
Risk profile
Behavioral economics
Bayesian inference
Structural health monitoring
Miter gates

ABSTRACT

This paper proposes an approach to select a maintenance strategy from a predefined set of choices considering the decision maker's behavioral risk profile. It is assumed that the damage state is characterized by a continuous state parameter probabilistically inferred from observable sensor data. This work applies an engineering application of consequence-based decision-making incorporating the acceptable risk intensity of the decision-maker, i.e., the decision-maker's (individual or an organization) valuation of the outcome of a decision, using a risk profile model. The utility of a decision-maker is subjective, and this paper considers the fact that different decision-makers mentally assign a different importance factor (the utility) to the seriousness or urgency to take necessary actions with the increasing intensity of structural damage. The approach herein incorporates a layer of human psychology on selecting appropriate maintenance strategies that not only depend on the posterior distribution of unmeasurable damage state but also consider the behavioral risk profile of the decision-maker. The collective decision-making of an organization consisting of many individuals is also investigated. The approach is exemplified in a case study involving life cycle monitoring of a miter gate, part of a lock system enabling navigation of inland waterways.

1. Introduction

Structural health monitoring (SHM) is the process of collecting in-situ data from an in-service structure and mining that data for information that informs decisions about the structure's state of health [1,2]. Such health information is then used for a variety of reasons typically related to operational or maintenance actions throughout the structure's life cycle. Due to the many sources of variability and/or noise that infuse this SHM "data-to-decision" workflow, the process of inferring the damage state from sensor measurements and making decisions regarding it is inherently probabilistic. A successful SHM workflow, therefore, requires in-situ data acquisition, feature extraction from the measurement data that will be used to perform the inference, probabilistic modeling of the features (and corresponding damage state), and subsequently evaluating some form of hypothesis on the features to make risk-informed decisions about the actions to be taken.

One of the most important classes of actions that SHM is designed to inform is maintenance planning. This paper focuses on risk-informed decision-making in SHM and proposes an approach to choose a series of maintenance actions (which may comprise an overall maintenance strategy) from a predefined set of choices, usually under the constraints of meeting a safety requirement and preserving cost-effectiveness. The maintenance actions constituting this set – the *decision space* – are assigned corresponding discrete labels, ratings, or indices that map to various degrees of damage relating to a limit state. As an example which will be exploited as a case study in this work, the U.S. Army Corps of Engineers (USACE) considers an operational conditional assessment (OCA) rating protocol consisting of five discrete damage labels: (*A* (excellent), *B* (good), *C* (fair), *D* (poor), *F* (failing), and *CF* (complete failure)) for its miter gate structures (discussed later in detail). These ratings are generally commensurate with increased overall damage state [3], and in turn the state parameters. In our present case study example, considering the monitoring and maintenance of USACE miter gate structures, the state parameter measuring "health" is a measure of the loss of boundary contact between the miter gate itself and its supporting wall quoin block at the bottom of the gate, hereafter referred to as the gap length. In the most unsophisticated case, the structure can be assigned a rating, which is used interchangeably with the term label, purely based on various mutually exclusive and collectively exhaustive ranges of true gap length values. For instance, the structure might be rated *A* if the true gap length value ranges

* Corresponding author.
E-mail addresses: machadha@ucsd.edu (M. Chadha), mramanch@ucsd.edu (M.K. Ramancha), mvegaloo@lanl.gov (M.A. Vega), jpconte@eng.ucsd.edu (J.P. Conte), mdtodd@eng.ucsd.edu (M.D. Todd).

https://doi.org/10.1016/j.ress.2022.108845
Received 13 September 2021; Received in revised form 16 September 2022; Accepted 18 September 2022
Available online 23 September 2022

from 0–30 inches; similarly, the structure might be rated *CF* for a gap greater than 180 inches [4]. This assignment could be made by either an inspector/engineer or organizationally determined by USACE; in either case, it may be informed by formal predictive limit-state analysis, prior expert experience, historical practice, or some combination.

Establishing maintenance policies usually has three major challenges. First, it requires establishing damage/state parameter(s) that is/are reflective of the structure's health. Unlike the demonstration problem that we consider in this paper, where the damage is quantified by a single well-defined damage parameter (gap length), it is usually not so straightforward to find these damage parameters and their relationship to the overall health of the structure. This requires running high-fidelity finite element models and obtaining macro/global damage parameters (or features). This paper assumes that the global/macro damage parameter(s) exist(s). Second, these damage parameters are continuous quantities that evolve with time and, for the purposes of establishing the maintenance policy, they require obtaining discrete structural health labels/ratings that are related to the damage parameter(s) (e.g., the OCA ratings A, B, C, D, F, and CF label in the case of the miter gate structure). If the labels are related to the damage parameter (gap value for the miter gate) as described in the simple example above, it is easy to define a unique maintenance action for each label (and consequently a strategy over the set of actions). However, such a simple label assignment system suffers from two major drawbacks: (1) it requires obtaining the exact value of the true damage parameter (like gap length value for the miter gate), which is typically impossible, and (2) it is a very rudimentary way of defining a label obtained by explicit discretization of the continuous state parameter. Third, having decided on the meaning of the indexing labels, the question then remains on how to design optimal maintenance policies for each of these labels.

As discussed in [5], in practice consequence-based decision-making often relies on subjective and experience-based expert elicitation of the probable structural state (usually defined by discrete labels). Such probabilistic assessments can be erroneous, especially when there is little to no prior experience or observation prior to a limit state such as catastrophic failure. Such assessments can lead to biased conservative and uneconomical maintenance decisions over the life of the structure. Furthermore, as discussed in [6], traditional conditioned-based maintenance practices require regular periodic inspections. In the initial to intermediate life of the structure, most inspections confirm that the structure does not need significant repairs. Therefore, it is crucial to develop a decision-making framework that is adaptive to the updated structural state to recommend necessary maintenance actions, and at the same time save cost by not recommending any unnecessary inspections, especially in the early operational life of the structure.

Inspection and maintenance planning is a very broad and widely researched area. Several contributions in the literature have focused their attention on building optimal inspection and maintenance planning for various structures subjected to different forms of damage like pipelines subjected to external corrosion [7], nuclear power plant steam generators subjected to multiple degradation mechanisms [8], water main breaks in distribution networks [9], systems subjected to stress corrosion cracking [10], optimal inspection planning for pipeline network [11], inspection model for defense and military systems [12], offshore wind turbine subjected to operational fatigue [13], railway track-bed maintenance [14], data-driven predictive maintenance for automobiles [15], to name a few. Establishing optimal inspection and maintenance policy initiates by building a physics-based model that is capable of simulating the structure's life cycle when subjected to varying environmental conditions. This allows for stimulating the degradation of the structure over time. Among all the choices of inspection and maintenance policies, an optimal maintenance strategy maximizes the benefit for the least cost. This entire process consists of four major steps: degradation modeling, maintenance effect modeling, maintenance policy elaboration, and performance assessment [16]. This requires investigating the impact of several policies on the degradation curve and estimation of remaining useful life. Needless to say that this entire process is computationally intensive. Recent progress in computational speed, and the application of Machine Learning on building a reasonably accurate digital twin for faster evaluation of degradation curves [17,18], has catalyzed research in numerous areas of optimal maintenance like condition-based maintenance policy [19], the impact of imperfect maintenance [20,21], impact of uncertain inspection data and condition rating protocol [4], maintenance planning multi-components system [22,23], inspection and maintenance for multi-state systems [24,25], maintenance for k-out-of-n systems [26,27], to name a few. The works by Fauriat et al. [28] and Lin et al. [29] utilize the Value of Information as a metric to guide the inspection policies such that the cost acquired over the life of the structure is minimal. Vega et al. [30] discuss the application of data analytics and machine learning to maintenance decision-making for civil infrastructure. Yang et al. [31,32] discuss optimal sensor design with the target of obtaining measurement data based on which a maintenance policy could be effectively implemented. The paper by Lam et al. [6] focuses on developing a decision-policy that considers the current structural health as an input to decide the future upcoming inspection.

In this paper, we focus on developing a framework where a finite number of maintenance actions are to be proposed and executed (each associated with a discrete label), but at the same time, the framework to design and choose the maintenance actions and overall strategy must account for the continuous and uncertain nature of the updated state parameter, as well as take into account the updated state of the structure (updated by utilizing the sensor measurements obtained through an SHM system). Another novelty of this paper is that it integrates the risk profile of the decision-maker (or the acceptable risk intensity that the organization demands, or by which the application is regulated), thereby quantifying the subjective component of decision-making. Proposing an integrated consequence-based decision-making framework is one of the primary focuses and contributions of this paper. We propose an approach to choosing a maintenance strategy on an economic basis that minimizes the consequence/regret of making a decision (i.e., choosing which maintenance action to pick among the available options) given the probability distribution of the inferred state parameter that indicates the degree of damage. Doing so requires three essential ingredients:

1. The first ingredient requires some bounding assumptions on the problem at hand. We assume that the state parameter sufficiently describes the degree of structural damage, and other than the state parameter, no other quantity is needed to describe the structural health (at least to the extent that it is assumed sufficient to make a decision and take an action). We also assume that the state parameter is unknown and is described by its probability density function. Therefore, the results and methodology presented in this paper are limited to such a class of problems where the state parameter is well-defined and continuous. Moreover, the demonstration problem considers a scalar state parameter. Therefore, the methodology presented is focused on a single state variable and could only in theory be extended to a multi-dimensional state parameter case. In the absence of any external maintenance, because the damage spontaneously and irreversibly increases over time, the state parameter must also have monotonically increasing (or decreasing, depending upon how it is defined) characteristics. To capture all the possible degrees of damage (the possible range of gap values in the present demonstration case), we need to consider the consequence of choosing a particular maintenance action for all the possible realizations of the state parameter. For example, choosing to do nothing (take no action) when the gap value for the miter gate is sufficiently large may be disastrous, whereas performing a costly repair when the gap value is sufficiently small is uneconomical. The *consequence cost* or *regret* function is uniquely defined for

each maintenance strategy and is essentially weights assigned to the damage intensity (or the true state parameter). The consequence cost function is arrived at for each maintenance action by estimating various costs associated with maintenance downtime, inspection, repair, replacement, and, in case of complete failure, life safety, and capital losses, and by investigating the state parameter evolution model using the high-fidelity finite element model.

2. The second ingredient is the requirement to arrive at the probability distribution of the state parameter. Since the state parameter is assumed to be only indirectly observable (the most generic case of all), it is probabilistically inferred from measurable sensor data using Bayesian inference.
3. Once the consequence cost functions for all the maintenance actions are defined, and once we have a reliable method to infer the posterior distribution of the state parameter, the third ingredient is the exploitation of expected utility theory to choose the optimal maintenance set of actions (refer to [33,34]). When the data is broadly available, the available data can be used directly to infer the probability distribution of the state parameter(s). For structural engineering applications such as the current case study where the experimental data is scarce (and unavailable in the damaged states), the posterior distribution of the state parameter may be obtained from a calibrated finite element model or a physics-informed digital surrogate using Bayesian inference [35]. We use a finite element model to generate the observable data (that is local strain gauge measurements) in this paper.

As a byproduct of optimally choosing a maintenance strategy, we also propose an approach to classify the structural state discretely. It is convenient for engineers to assess the state of the structure discretely (e.g., undamaged, moderately damaged, and critically damaged). For simple problems where the possible discrete states of the structure have well-defined physical definitions and sufficient examples of all realized states, the state assessment is done using a statistical classifier, i.e., a typical detection type problem. Defining the classifiers objectively requires a large amount of data (more specifically, features) that span the target damage states of interest, and supervised learning may be employed to define the classifiers. However, unlike a well-defined detection type problem encountered in data science, objectively defining a mutually exclusive and exhaustive set of discrete structural states is challenging since the structure evolves continuously and the state of the structure is inherently a continuous quantity. In the case of the SHM system installed on a complex structure with numerous sensors and a continuous degree of damage, such objective well-defined classifiers may not necessarily be obtainable. This is because, in practice, features are very unlikely to be obtained in all possible classification states (especially higher damage or failed states). We tackle this limitation by exploiting the fact that each maintenance action is associated with or designed for a label that represents a level of damage. These labels can be used as a proxy for discrete state classifiers. We exploit the following facts: (a) unlike a structural state that is inherently a continuous quantity, the maintenance strategies are countable; (b) the consequence cost function associated with each maintenance action label is implicitly designed by considering a level of damage; thus, choosing an optimal maintenance strategy allows us to reasonably use the associated labels as a proxy to discrete state classifiers.

Although the consequence cost function for a set of maintenance actions may be estimated reasonably by the structural asset owner/operator, the actual decisions made are inherently affected by the biases and heuristics of the decision-maker (e.g., an inspection engineer) or are risk-weighted [36]. Not only is the behavioral risk profile of an individual decision-maker affected by his/her biases, but also by any organizational values and priorities. Additionally, as discussed in [37], although difficult to precisely define, an organization has a risk profile based on its alignment with values, priorities, or regulations. For example, high-consequence organizations like nuclear power plants must be extremely *risk-averse* towards danger of core meltdown due to high public safety consequences (see [38]). A well-designed SHM system can be instrumental in obtaining reliable *information* regarding structural health. However, utilizing this information to select the course of action depends on the qualification, competence, and experience of the engineer as well as the values, priorities, and guidelines set by an organization or regulations by which the organization must abide.

This decision-making scenario under uncertainty motivates us to model and investigate the effect of decision-maker's risk profile on decision-making. We achieve this by accounting for the decision-maker's utility, i.e., the their evaluations about the outcome of an action, using risk profiles in the decision-making process. The utility of a decision-maker is subjective and hence considers the fact that different decision-makers mentally assign a different importance factor (or in economic terms, the utility or risk-intensity) to the seriousness or urgency of a given state in order to take necessary actions commensurate with the intensity of structural damage. The approach herein incorporates a layer of human psychological behavior on selecting appropriate maintenance strategies that not only depend on the structural state (probabilistically quantified by the posterior distribution of the damage parameter) but also consider the risk profile of the interpreting decision-maker(s). In the case of an organization, which might be comprised of many decision-makers, we also investigate the collective decision-making behavior of the organization. The collective performance of the organization depends on the distribution of the risk profiles of the agents it employs (which in turn are impacted partly by the organization's values, policies, and decision-making guidelines). This paper does not elaborate on ways to psychologically evaluate and define an individual's risk profile, nor does it detail a methodology to evaluate the risk profile of an organization; such a thing is based on a complex array of its values, motto, operational capabilities, overall competency of the management, the negative impact of bureaucracy and loss of productivity in the case of large organizations, experience and qualification of the employees, and corporate greed, to name a few (see [37]). We approach this problem by modeling the spectrum of risk profiles (or utility functions) of various decision-makers that form the organization and investigating the impact of different cases of risk intensities on decision-making. Assuming that an organization is as good as its employees in an average sense, the organizational risk profile is then defined based on the weighted average consequences of the decisions made by the employees.

Decision theory enjoys a very rich history (refer to [39]) that dates back to the work in probability theory by Blaise Pascal and Pierre de Fermat, and the work of Bernoulli [40] on decision-making under uncertainty. As demonstrated by the Petersburg paradox (see Chapter 7 of [41]), people do not maximize expected monetary value while making decisions. Bernoulli [40] suggested that the decision-maker maximizes the expected value of a cardinal utility function that represents the strength of preference for certain outcomes. The sound theoretical foundation of expected utility theory lies in the work of John von Neumann and Oskar Morgenstern [33] on game theory and economic behavior. However, the expected utility theory assumed that the decision-makers are rational. This theory was extended to *prospect theory* (a theory of the psychology of choice) and finally to *cumulative prospect theory* (a model for descriptive decision under risk and uncertainty) by Amos Tversky and Daniel Kahneman [42,43] who also included the irrationality and heuristic biases of the decision-maker.

Many engineering applications involve decision-making under uncertain, risk-bearing scenarios. Several research efforts have been made to adopt the expected utility theory and other decision-making models in decision analysis for engineering applications. A paper by Gardoni et al. [44] mentions that most engineering decision-making is mathematically modeled through three different methods: *life cycle cost analysis*, *expected utility theory*, or *cumulative prospect theory*. As is one

of the main focuses of this paper, Gardoni et al. [44] points to the fact that the decision-maker's preference and risk behavior plays a crucial role in the outcome of decision analysis. A number of works [45,46] dealt with considering and modeling risk-aversiveness in the decision-making process. Faber et al. [47–50] investigated the decision-making under uncertainty in SHM and structural reliability problems. More recently, approaches quantifying the economic benefit of using an SHM system (refer to [51–54]) have been investigated by using *value of information* theory [55] in conjuncture with expected utility theory. Bolognani et al. [56] extend the application of prospect theory to include irrationality in decision-making for the SHM application.

As far as the applications of probability theory are concerned within the field of civil engineering, the readers are referred to an excellent book (especially the last two chapters) by Benjamin and Cornell [57]. We cautiously note that in this paper, we stick to the expected utility framework and incorporate the risk-perception of the decision-makers using a non-linear logarithmic utility function.

As introduced above, we consider for our case study a miter gate structure, an important component of the lock systems used for inland waterway navigation [58,59]. The USACE spends billions of dollars in maintaining and operating this infrastructure, where the unscheduled shutdown of these assets and dewatering for inspection or repair is very costly [3,60,61]. The potential for SHM to help facilitate maintenance and operations appears highly promising. Within the navigation lock systems, miter gates are one of the most common locking gates used; their most common failure mechanisms include long-term corrosion and loss of load-transferring contact in the quoin block, as discussed above [62]. As many of these structures have been operational for over 50 years, many are presently potentially operating with higher risk without engineers knowing their real structural residual strength capacity; current practice involves engineering elicitation via inspection, followed by lock closures if the inspection so warrants. Since this process is based on the varied experience and interpretation of field engineers, it bears high uncertainty and variability [63]. The use of an SHM system coupled with a framework that decides an optimal maintenance strategy considering the various levels of risk intensity could lead to reduced life cycle costs including an effective increase in remaining useful life. We note that each engineering-based decision-making problem requires customized rules/policy that considers the problem at hand. Therefore, the proposed framework is focused on the application of consequence-based decision-making for miter gate structures and the principles can only, in theory, be extended to other more complex problems.

The rest of the paper is arranged as follows. Section 2 reviews the general framework of expected utility theory. Section 3 describes the demonstration case study and general decision-making framework that we propose. Section 4 first describes the maintenance actions and their associated consequence cost functions, and then it details the individual and organizational risk profiles. Section 5 presents posterior decision analysis to determine the maintenance strategy and label the structure considering individual and organizational risk behavior. Finally, Section 6 concludes the paper.

2. Consequence-based decision-making framework

Consider an SHM based decision-making problem where the decision to be made (like choosing a maintenance action) depends on the uncertain state parameter(s) denoted by a random variable Θ and defined over the state-parameter space Ω_Θ. The *decision space* (for example: set of different maintenance actions, or equivalently, the set of the corresponding damage labels) is represented by Ω_D. In general, Ω_D and Ω_Θ can be discrete or continuous. However, suitable to the present application, we assume that the decision space Ω_D and the state parameter(s) space Ω_Θ are discrete and continuous, respectively, such that $\Omega_D = \{d_0, d_1, \dots, d_n\}$ and $\theta \in \Omega_\Theta$. Here, the elements of Ω_D, i.e., $d_i \in \Omega_D$ for $i \in \{1, 2, \dots, n\}$, represent a damage label that has a corresponding maintenance action associated with (or designed for) it. We attempt to answer the question: *For a given probability distribution of the state parameter(s), what rating must be assigned to the structure that leads to an optimal maintenance strategy?*

To answer this question directly, we first define uncertainty in state parameter(s) θ by its probability density function $f_\Theta(\theta)$. Let θ_{true} represent the *true value(s) of state parameter(s)*, and we assume that they cannot be measured. The numerical value of θ_{true} falls in the domain Ω_Θ. To predict the optimal decision, we need to minimize average loss or expected risk (also called the Bayes risk functional) arising as a consequence of making the decision. To arrive at Bayes risk, we define *consequence/regret cost function* $L\left(d_i, \theta_{\text{true}}\right)$ that defines the total loss or regret as a consequence of making decision d_i considering all the possible values of true state parameter(s) $\theta_{\text{true}} \in \Omega_\Theta$. It gives an *extrinsic cost* involved with decision-making. The expected loss or the Bayes risk Ψ_{prior} is then defined as

$$\begin{aligned}\Psi_{\text{prior}}(d_i) &= E_\Theta\left[L\left(d_i, \theta_{\text{true}} = \theta\right)\right] \\ &= \int_{\Omega_\Theta} L\left(d_i, \theta_{\text{true}} = \theta\right) f_\Theta(\theta)\, \mathrm{d}\theta, \forall i \in \{1, 2, \dots, n\}.\end{aligned} \tag{1}$$

The optimal decision, denoted by $\mathscr{d}_{\text{prior}} \in \Omega_D$, is the one that minimizes the Bayes risk, or

$$\mathscr{d}_{\text{prior}} = \underset{d_i}{\operatorname{argmin}}\, \Psi_{\text{prior}}(d_i). \tag{2}$$

We observe that $f_\Theta(\theta)$ embeds our prior knowledge of state parameter(s) θ before any additional information is available (for example, obtained using sensors in SHM). Obtaining the optimal decision using Eq. (2) is called a *prior decision analysis*.

We now consider a scenario where additional information (sensor measurements) is available. For sake of argument, we assume that new information is obtained by a mechanism z (for example an SHM system). The newly acquired measurements are assumed to be uncertain as the sensor data is subjected to noise. Therefore, in the Bayesian viewpoint, sensor measurements are modeled as a random variable, denoted by X_z. Let Ω_{X_z} represent continuous measurement space, such that $x_z \in \Omega_{X_z}$, where x_z is a realization of the random variable X_z. The subscript z denotes the mechanism by which new information was acquired. Installing information gathering system incurs an *intrinsic cost* $C(z)$. Therefore, sum total of the extrinsic and the intrinsic cost functions $L_z(d_i, \theta_{\text{true}}) = C(z) + L(d_i, \theta_{\text{true}})$ is used for further decision analysis. With the availability of additional information, we define Bayes risk Ψ_z for posterior decision analysis as:

$$\begin{aligned}\Psi_z(d_i) &= E_{\Theta X_z}\left[L_z(d_i, \theta_{\text{true}})\right] = E_{X_z}\left[E_{\Theta|X_z}\left[L_z(d_i, \theta_{\text{true}} = \theta)\right]\right] \\ &= \int_{\Omega_{X_z}} f_{X_z}(x_z) R_z(d_i; x_z)\, \mathrm{d}x_z;\end{aligned} \tag{3}$$

where,

$$R_z(d_i; x_z) = E_{\Theta|X_z}\left[L_z(d_i, \theta)\right] = \int_{\Omega_\Theta} L_z(d_i, \theta_{\text{true}} = \theta) f_{\Theta|X_z}(\theta|x_z)\, \mathrm{d}\theta. \tag{4}$$

In the equation above, $R_z(d_i; x_z)$ represents *conditional risk*. It represents expected value of loss as a consequence of making a decision considering the posterior distribution of state parameter(s) $f_{\Theta|X_z}(\theta|x_z)$ (*conditioned* on new information acquired through the mechanism z) which is essentially the updated distribution of state parameter(s) θ after new information x_z is available. With this understanding, we can write the Bayes risk and the optimal decision $\mathscr{d}_z$ as

$$\Psi_z(d_i) = E_{X_z}\left[R_z(d_i; x_z)\right]; \tag{5a}$$

$$\mathscr{d}_z = \underset{d_i}{\operatorname{argmin}}\, R_z(d_i; x_z). \tag{5b}$$

We assume that the new information should be such that it brings an observer closer to the true state parameter(s) relative to what was reflected in the prior knowledge of state parameter(s). With this assumption, the decision obtained using Eq. (5) is better than the

decision obtained by prior analysis using Eq. (2) because additional information x_z reduces uncertainty and brings one closer to the true state parameter(s). Utilizing equation set (5) to obtain the optimal decision is referred to as *posterior decision analysis*. The subscript $(.)_{\text{prior}}$ and $(.)_z$ in Bayes risk and optimal decision are meant for prior and posterior decision analysis (using information obtained through the mechanism z), respectively.

The posterior probability distribution $f_{\Theta|X_z}(\theta|x_z)$ remains to be evaluated. We realize that the posterior $f_{\Theta|X_z}(\theta|x_z)$ is non-causal. State parameter(s) can be thought of as a *cause* with measurement being its *effect*. In this regard, inferring the state parameter(s) (cause) given the measurement (effect) is non-causal. We use Bayes theorem to write $f_{\Theta|X_z}(\theta|x_z)$ in a more desirable and causal form:

$$f_{\Theta|X_z}(\theta|x_z) = \frac{f_{X_z|\Theta}(x_z|\theta)f_\Theta(\theta)}{f_{X_z}(x_z)} = \frac{f_{X_z|\Theta}(x_z|\theta)f_\Theta(\theta)}{\int_{\Omega_\Theta} f_{X_z|\Theta}(x_z|\tau)f_\Theta(\tau)\mathrm{d}\tau}. \tag{6}$$

As discussed before, the likelihood $f_{X_z|\Theta}(x_z|\theta)$ is relatively easier to calculate than the posterior $f_{\Theta|X_z}(\theta|x_z)$. The likelihood can be easily obtained using the forward simulated model of the system that yields x_z for a given value of θ (for example, the finite element model yielding measurements x_z for a given damage level θ). Alternatively, the measurements x_z can be obtained for various instances of the damage parameter θ experimentally. The data set (x_z, θ) obtained through a lab-based experimental testing can then be used to obtain the likelihood $f_{X_z|\Theta}(x_z|\theta)$. Numerical techniques like Markov Chain Monte Carlo (MCMC), and Sequential Monte Carlo (SMC), or transitional MCMC [64] can be used for Bayesian inference. The following section presents and discusses the demonstration problem concerning the miter gate structure.

3. Demonstration problem

3.1. Problem description

To demonstrate the application of concepts discussed so far, we consider an example problem of the Greenup miter gate maintained and managed by USACE located on the Ohio River, USA. Fig. 1 shows a lock and the miter gate system (image adapted from the USACE website and Eick et al. [65]). Loss of contact between the vertical side of a gate and the supporting concrete wall (boundary-related damage) is the most commonly observed damage mechanism in such systems [3,62,63]. This loss of contact is manifested by the formation of a gap between the gate and the wall quoin blocks at bottom of the gate. The amount (or length) of this loss of contact is referred to as *gap length* in this paper. Therefore, we treat the gap length as a scalar continuous state parameter $\theta \in \Omega_\Theta$ (refer to Fig. 2), such that $\Omega_\Theta = [\theta_{\min}, \theta_{\max}]$. Here, $\theta_{\min}$ is the lower bound of the gap length, and $\theta_{\max}$ is the upper bound of the gap length which indicates that the gate is critically damaged and failure is imminent. This value is suggested by the USACE engineers based on their experience and past inspection data. In many cases, data related to the failure of the structure may not be available because the decision-makers are risk-averse and they do not want to see a gap length large enough leading to failure. In such scenarios, a physics/mechanics-based high-fidelity numerical simulation should be performed to estimate $\theta_{\max}$. Based on feedback from USACE field-engineers [62], the upper bound of the gap length can be considered as $\theta_{\max} = 180$ inches for gates that have similar structural characteristics as the Greenup miter gate. If no value of $\theta_{\min}$ is specified, it can be taken as 0 in (indicating pristine state of the gate). Unlike non-binary rating protocols used by USACE, i.e. (*A, B, C, D, F,* and *CF*), to build our framework, we use a rather simplified binary labeling system that consists of two discrete damage labels/index of the miter gate, such that the decision space reduces to $\Omega_D = \{d_0, d_1\}$, where the binary decisions are

$$\begin{aligned} d_0 &: \text{label indicating that the gate is undamaged with} \\ &\quad \text{excellent operational capacity,} \\ &\quad \text{and requires no maintenance;} \\ d_1 &: \text{label indicating that the gate is damaged,} \\ &\quad \text{is not safely operational,} \\ &\quad \text{and requires maintenance.} \end{aligned} \tag{7}$$

The physical location of the gap appearance is in part of the gate that is always submerged underwater during operational conditions. Therefore, loss of contact length cannot be directly observed and measured during operational conditions, and the gap length becomes our unknown parameter. This unknown parameter can be estimated (or inferred) from other indirect measurements of some kind available at distributed locations on the structure. The Greenup miter gate is equipped with an array of strain gauges indicated by red dots in Fig. 2. These strain gauge readings are recorded in real-time and are used as the set of measurements that will be used to infer the gap length. We simulate our data acquisition process using a detailed high-fidelity finite element model (FEM) of the Greenup miter gate previously validated in the undamaged condition of the gate with available actual strain gauge readings [62]. When the miter gate is first deployed, the gap length is reasonably assumed to be zero, under the assumption of no deployment problems. A FEM of the pristine miter gate needs to be constantly updated (as a live digital twin) as and when new information from the strain gauge sensor array is obtained. Because a very limited amount of actual data is available from Greenup, we turn to a physics/mechanics-based FEM of the miter gate (see Fig. 2) as the ground truth surrogate for data. In that regard, we assume that there are no measurement biases and that the sensor readings are subject to random unbiased noise. As with any such model, its representative predictive value is only as good as its validation based on the real structure that it represents. In this case, the FEM was previously validated for the Greenup miter gate in the undamaged condition, as mentioned earlier, but modeling of damage formation of the gap itself could not be validated on actual data from the gate in a known damaged condition, so modeling bias error in the damage state could creep into the process. That does not change or otherwise invalidate the demonstration of the proposed approach or its utility, but rather it provides caution on interpreting the specific results for this case beyond the demonstration of the overall approach. Since the data is acquired from the strain-gauge array constituting the SHM system, from here on, z denotes the SHM system. The posterior distribution $f_{\Theta|X_z}(\theta|x_z)$ of the gap length given the strain sensor measurements is then obtained using Bayesian inference discussed in the next Section 3.2. Here, X_z denotes a random variable that represents the measurement obtained from the sensors deployed in the SHM system, with Ω_{X_z} representing the space of those measurements.

3.2. Inferring the gap length using Bayesian inference

As discussed in the previous section, the state parameter is the gap length θ, and the measurement vector $x_z \in \Omega_{X_z}$ is the strain recorded at $N_{\text{sg}}(z)$ number of strain gauges. Therefore, X_z is a random vector. The red dots in Fig. 2 show the locations of the $N_{\text{sg}}(z) = 46$ strain gauges considered for the simulation. The measurements obtained from the strain-gauges are used to infer the gap length θ using Eq. (6) that we recall below for the sake of continuity

$$f_{\Theta|X_z}(\theta|x_z) = \frac{f_{X_z|\Theta}(x_z|\theta)f_\Theta(\theta)}{f_{X_z}(x_z)}. \tag{8}$$

In the equation above, $f_\Theta(\theta)$ is the prior probability distribution, $f_{X_z|\Theta}(x_z|\theta)$ is the likelihood function, and $f_{\Theta|X_z}(\theta|x_z)$ is the posterior

Fig. 1. An example of a lock and miter gate system.

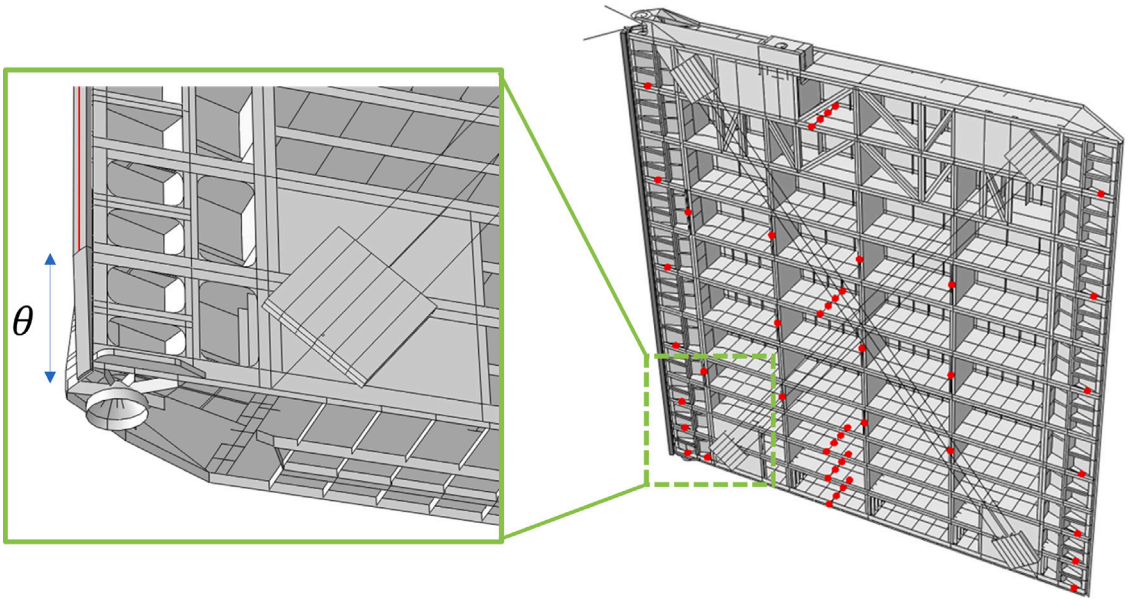

Fig. 2. Physics-based model of miter gate and the bearing gap.

probability distribution that needs to be evaluated. In the context of inferring θ, the evidence $f_{X_z}(x_z)$ is just a normalizing constant. Therefore, Eq. (8) can be written as

$$f_{\Theta|X_z}(\theta|x_z) \propto f_{X_z|\Theta}(x_z|\theta) f_\Theta(\theta). \tag{9}$$

The distribution $f_\Theta(\theta)$ reflects the prior knowledge about the parameter θ before any new information (or measurements) are obtained. Assuming only basic geometric constraints on the gap length, we assume the prior gap length to be a uniform distribution spanning over $\Omega_\Theta = [\theta_{\min}, \theta_{\max}]$, such that

$$f_\Theta(\theta) = \begin{cases} (\theta_{\max} - \theta_{\min})^{-1} & \theta \in \Omega_\Theta; \\ 0 & \text{otherwise.} \end{cases} \tag{10}$$

To evaluate the posterior distribution using Eq. (9) requires the likelihood function. Constructing the likelihood function $f_{X_z|\Theta}(x_z|\theta)$ requires a model of the measurement process. In this paper, we use the following measurement model

$$x_z = h_z(\theta_{\text{true}}, u) + w_z. \tag{11}$$

In the equation above, $x_z = (x_{z1}, x_{z2}, \ldots, x_{zN_{\text{sg}}(z)}) \in \Omega_{X_z}$ is a realization of the random vector X_z consisting of $N_{\text{sg}}(z)$ static strain measurements for a given water heads at each side of the miter gate, where x_{zi} represents the strain value corresponding to the ith strain gauge. The quantity $h_z(\theta, u)$ defines the *true* strain gauge array response obtained by the finite element model for the true gap-length value θ_{true} when subjected to the input loading u (consisting of upstream and downstream water heads), such that $h_z(\theta_{\text{true}}, u) = (\hbar_{z1}(\theta_{\text{true}}, u), \hbar_{z2}(\theta_{\text{true}}, u), \ldots, \hbar_{zN_{\text{sg}}(z)}(\theta_{\text{true}}, u))$. Here, $\hbar_{zi}(\theta_{\text{true}}, u)$ represents the true strain value of the ith strain gauge when the true gap-length value is θ_{true} and u is the input loading. The input loading $u = (h_{\text{up}}, h_{\text{down}})$ consists of the hydro-static load on the gate, where h_{up} and h_{down} represents the hydro-static head in the upstream and the downstream respectively. Finally, the random vector W_z with a realization $w_z = (w_{z1}, \ldots, w_{zN_{\text{sg}}(z)})$ represent the measurement noise/error vector, where w_{zi} denotes the error between the measurement output and finite element predicted response corresponding to the ith strain gauge. We assume that W_z follows a zero-mean Gaussian distribution with independent components, i.e., the noise/error terms of all $N_{\text{sg}}(z)$ strain gauges are assumed to be statistically independent. In addition, we assume that all strain gauges have the same noise/error standard-deviation σ_{strain}, such that

$$f_{W_z}(w_z = (w_{z1}, \ldots, w_{zN_{\text{sg}}(z)})) = \prod_{i=1}^{N_{\text{sg}}(z)} \phi\left(\frac{w_{zi}}{\sigma_{\text{strain}}}\right). \tag{12}$$

Using the measurement model defined in Eq. (11), and the description of noise in Eq. (12), the likelihood can be written as

$$f_{X_z|\Theta}(x_z|\theta) = \prod_{i=1}^{N_{sg}(z)} \phi\left(\frac{x_{zi} - \hbar_{zi}(\theta, u)}{\sigma_{\text{strain}}}\right). \tag{13}$$

Having defined the prior distribution and the likelihood function in Eq. (10) and (13), we note that the posterior distribution cannot be obtained analytically using Eq. (8). This is because the relationship between the gap length θ and the strain measurements x_z is highly nonlinear and only available numerically through the finite element simulation. One can rely on numerical approximation techniques like Markov chain Monte Carlo (MCMC) methods or sequential Monte Carlo (SMC) methods to solve the inference problem (refer to [64,66–68]). However, these numerical techniques demand evaluation of the likelihood function $f_{X_z|\Theta}(x_z|\theta)$ at numerous values of θ. Evaluating the likelihood using Eq. (13) at each value of θ requires running the finite element model h_z. Thus, the process of Bayesian inference becomes extremely computationally expensive while using high-fidelity finite element models, such as in this work. Consequently, we employ the transitional Markov chain Monte Carlo (TMCMC) algorithm to perform Bayesian inference. The inherent architecture of the TMCMC algorithm allows for parallel computing and hence is ideal for inference when dealing with computationally expensive high-fidelity FE models. The algorithmic details of the TMCMC can be found in [64,67–69]. Besides, TMCMC has been applied to the miter gate model in [66]. Note that the TMCMC algorithm is closely related to the class of SMC algorithms.

We simulate strain measurement data numerically. For simulating such data, we obtain response of the FE model $h_z(\theta_{\text{true}}, u)$ parameterized by a fixed chosen value of θ_{true} subjected to a fixed chosen input loading $u = (h_{\text{up-true}}, h_{\text{down-true}})$. The finite element strain response is now corrupted with zero-mean Gaussian noise of standard deviation $\sigma_{\text{strain-true}}$ to simulate strain measurement noise. This noise corrupted finite element response is now used as the measurement data x_z. For the posterior analysis in Section 5, we consider five sets of measurement data resulting in five cases of a posterior distribution. Parameter values used to simulate five sets of measurement data are shown in Table 4. During inference, it is assumed that the input loading corresponding to each of these cases (cases 1–5) is known accurately, i.e., $h_{\text{up}} = h_{\text{up-true}}$, and $h_{\text{down}} = h_{\text{down-true}}$. This is a valid assumption since the height of water upstream h_{up} and downstream h_{down} can be easily measured with fairly high certainty. On the other hand, the standard deviation of measurement noise σ_{strain} is extremely difficult to quantify accurately when using real measurement data. To mimic this real-world scenario, σ_{strain} in Eq. (12) is set to some non-true value for each case while inferring the gap length θ, i.e., $\sigma_{\text{strain}} \neq \sigma_{\text{strain-true}}$ for each case.

4. Cost function and risk profiles

4.1. Maintenance actions

Let M_0 and M_1 represent the actions associated with the labels d_0 (rating the structure as undamaged) and d_1 (rating the structure as damaged), respectively. That is, if the structure is labeled/rated as d_i, with $i \in \{0, 1\}$, then we perform the maintenance M_i, such that

$$\begin{aligned} &M_0 : \text{Do nothing;} \\ &M_1 : \text{Shutdown, inspect, and repair or replace} \\ &\quad \text{if required based on the inspection results.} \end{aligned} \tag{14}$$

Choosing either M_0 or M_1 will have an associated consequence cost depending on what the true state of the structure is. For instance, choosing M_0 for a newly-constructed gate (with the true gap length value being zero or negligibly small) is obviously an optimal decision. On the other hand, the same maintenance action M_0 can lead to catastrophic consequences when the true value of gap length is close to $\theta_{\max}$ (implying a heavily damaged gate near critical failure). Similarly, choosing M_1 for a pristine gate is unnecessary, while it may be an optimal decision when the gate is approaching critical failure (with a larger value of the true gap length). The next section proposes the base consequence cost functions.

4.2. Base consequence cost function

Tversky [70] noted that in order to simplify the choice between alternatives, people often disregard components that the alternatives share and focus on the components that distinguish them, a phenomenon referred to as the *isolation effect* [42]. The isolation effect also implies that the carrier of value is the change of wealth, rather than final asset positions that include current wealth, the observation first made by Markowitz [71]. In the maintenance action selection problem at hand, the *isolation effect* translates to the fact that when designing the consequence cost function, we only consider the consequence of choosing a particular action and ignore the current value of the asset. Since our decision-making preferences depend on this relative change in value, we use the consequence cost in *isolation* to (or by ignoring) the current value of the asset (the miter gate).

Recall the prior and posterior decision-making using Eqs. (2) and (5a), respectively. Since the state parameter is described probabilistically, it is necessary to consider all the possible realizations of the state parameter in the decision-making process. This is achieved by evaluating the value of Bayes risk for each choice of maintenance actions as an expected value of consequence cost. Let $L(d_0, \theta_{\text{true}})$ and $L(d_1, \theta_{\text{true}})$ denote the consequence costs of performing the maintenance actions M_0 and M_1, respectively, where the true degree of damage is defined by θ_{true}. The *consequence cost* or *regret* function $L(d_i, \theta_{\text{true}})$ is defined for each maintenance strategy M_i (corresponding to the label d_i) and it weighs an impact of choosing a maintenance action M_i for all the possible true degrees of damage $\theta_{\text{true}} \in \Omega_\Theta$. For example, choosing to do nothing (M_0) when $\theta_{\text{true}} = 100$ inches is more consequential than doing nothing (M_0) when $\theta_{\text{true}} = 50$ inches. That is, $L(d_0, \theta_{\text{true}} = 100 \text{ inches}) > L(d_0, \theta_{\text{true}} = 50 \text{ inches})$.

The functional form of the consequence cost function $L(d_0, \theta_{true})$: In the absence of any external action or maintenance (i.e., M_0), the damage of the structure is a spontaneous and irreversible thermodynamic process [72]. Therefore, for M_0, the consequence function $L(d_0, \theta_{\text{true}})$ should assign a higher relative consequence weights for a higher relative damage level. That is, $L(d_0, \theta_{\text{true}})$ should have monotonically increasing functional form. We assume that the consequence cost $L(d_0, \theta_{\text{true}})$ bears a linear functional form (simplest form of monotonically increasing function) bounded by the cost of doing nothing for the extreme cases of damage.

The functional form of the consequence cost function $L(d_1, \theta_{true})$: Action M_1 is a sequential maintenance strategy. A simple example of the maintenance strategy M_1 might be:

$$M_1 = \begin{cases} \text{Shutdown, inspection, and no repairs} & \theta_{\text{true}} \in [\theta_{\min}, \theta_1) \\ \text{Shutdown, inspection, and minor repairs} & \theta_{\text{true}} \in [\theta_1, \theta_2) \\ \text{Shutdown, inspection, and moderate repairs} & \theta_{\text{true}} \in [\theta_2, \theta_3) \\ \text{Shutdown, inspection, and major repairs/replacement} & \theta_{\text{true}} \in [\theta_3, \theta_{\max}] \end{cases}$$

Due to the sequential nature of M_1, its cost increases as the damage intensity increases. An appropriate functional form for the consequence function $L(d_1, \theta_{\text{true}})$ would be a piecewise increasing step function. Instead of evaluating the costs to these sequential actions, we simply evaluate the cost to perform the maintenance M_1 when the gate is

Table 1
Decision cases and their consequence-costs for the extreme values of the gap length θ_{true}.

	True state parameter $\theta_{\text{true}} = \theta_{\min}$	True state parameter $\theta_{\text{true}} = \theta_{\max}$
Label/Rating: d_0 Action: M_0	$L(d_0, \theta_{\min}) = \alpha_{\min}$	$L(d_0, \theta_{\max}) = \alpha_{\max}$
Label/Rating: d_1 Action: M_1	$L(d_1, \theta_{\min}) = \beta_{\min}$	$L(d_1, \theta_{\max}) = \beta_{\max}$

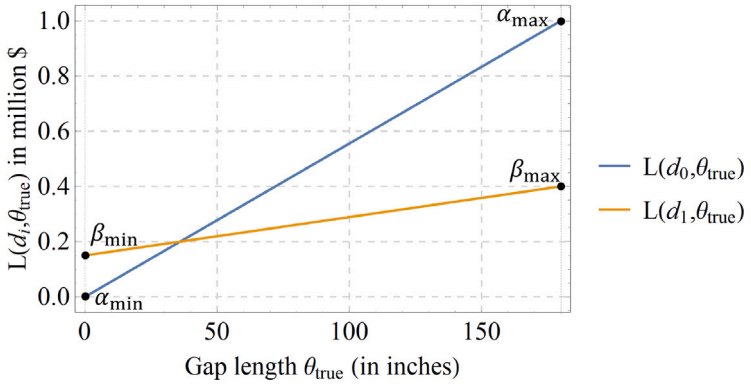

Fig. 3. Cost functions $L(d_i, \theta_{\text{true}})$, $i \in \{0, 1\}$.

undamaged (i.e., $L(d_1, \theta_{\text{true}} = 0)$), and for the case when the gate is damaged (i.e., $L(d_1, \theta_{\text{true}} = 180$ inches)). The consequence of performing maintenance M_1 for any generic value of θ_{true} is approximately estimated by a linear function bounded by the consequence costs for extreme cases of damage.

Consequence cost for extreme cases of damage: We estimate the real cost for both the maintenance strategies considering the extreme values of true gap length ($\theta_{\text{true}} = \theta_{\min} = 0$ inches and $\theta_{\text{true}} = \theta_{\max} = 180$ inches). We do this because the extreme values of the gap have interpretable physical meaning. The value of $\theta_{\text{true}} = 0$ inches indicates that the gate is pristine, and the value of $\theta_{\text{true}} = 180$ inches indicates that the gate is severely damaged and a critical failure is incipient. Under such damage conditions, the economical consequence of choosing a maintenance action can be reasonably evaluated since the consequences of decision-making are well-defined. When the gap length is zero, or $\theta_{\text{true}} = \theta_{\min} = 0$ inches, the gate is in pristine condition. Therefore, for $\theta_{\text{true}} = 0$ inches, rating the gate as undamaged, or d_0, and *doing nothing* (or choosing action M_0) is an optimal decision and costs nothing, i.e. $L(d_0, 0) = \alpha_{\min} = 0$. However, for a pristine gate, performing the action M_1 leads to unnecessary cost (denoted by $L(d_1, 0) = \beta_{\min}$) due to *down-time economic losses* and *inspection costs*. Once the pristine condition of the gate is established as a result of inspection, no repairs are carried out. Following along a similar line of reasoning, we consider another extreme end of gap length value of $\theta_{\text{true}} = \theta_{\max} = 180$ inches that reflects a severely damaged gate. Choosing the action M_0 for such a severely damaged gate can lead to consequence costs due to structural failure, loss of life and property, and the cost of replacement, denoted collectively by $L(d_0, \theta_{\max}) = \alpha_{\max}$. This damage state of the structure demands optimal maintenance to be M_1 leading to costs associated with *down-time economic losses, inspection costs* and *major repairs/replacement costs*, collectively denoted by $L(d_1, \theta_{\max}) = \beta_{\max}$. In addition to the cost $L(d_1, 0)$, the cost $L(d_1, \theta_{\max})$ includes an additional expense of major repair or replacement. Therefore, $L(d_1, \theta_{\max}) > L(d_1, 0)$. However, the most expensive decision is choosing to do nothing when the gate is critically damaged, making $L(d_0, \theta_{\max})$ the maximum cost among the four cases discussed here, such that, $L(d_0, \theta_{\max}) > L(d_1, \theta_{\max}) > L(d_1, 0) > L(d_0, 0)$, or $\alpha_{\max} > \beta_{\max} > \beta_{\min} > \alpha_{\min}$.

Base consequence cost functions: For each maintenance case, we have two objectively defined consequences at $\theta_{\text{true}} = \theta_{\min}$ and $\theta_{\text{true}} = \theta_{\max}$. A linear consequence cost has following form:

$$L(d_i, \theta_{\text{true}}) = C_{i0} + C_{i1}\theta_{\text{true}}. \tag{15}$$

We obtain the constants C_{i0} and C_{i0} using the constraints listed in Table 1. The consequence cost (illustrated in Fig. 3) functions are obtained as:

$$\begin{aligned} L(d_0, \theta_{\text{true}}) &= C_{00} + C_{01}\theta_{\text{true}} \\ &= \left(\frac{\theta_{\max}\alpha_{\min} - \theta_{\min}\alpha_{\max}}{\theta_{\max} - \theta_{\min}}\right) + \left(\frac{\alpha_{\max} - \alpha_{\min}}{\theta_{\max} - \theta_{\min}}\right)\theta_{\text{true}}; \\ L(d_1, \theta_{\text{true}}) &= C_{10} + C_{11}\theta_{\text{true}} \\ &= \left(\frac{\theta_{\max}\beta_{\min} - \theta_{\min}\beta_{\max}}{\theta_{\max} - \theta_{\min}}\right) + \left(\frac{\beta_{\max} - \beta_{\min}}{\theta_{\max} - \theta_{\min}}\right)\theta_{\text{true}}. \end{aligned} \tag{16}$$

Since $\alpha_{\max}$ is the maximum extreme cost, the costs $\beta_{\min}$ and $\beta_{\max}$ can be expressed as a fraction of $\alpha_{\max}$. For the purposes of numerical simulation in this paper, we assume $\beta_{\min} = 0.15\alpha_{\max}$ and $\beta_{\max} = 0.4\alpha_{\max}$. We assign a dollar value of \$1 million to $\alpha_{\max}$. Under this assignment, Fig. 3 gives the cost functions $L(d_0, \theta_{\text{true}})$ and $L(d_1, \theta_{\text{true}})$.

Remark 1. Treating the SHM-informed decision-making as a typical data-science based *traditional detection/classification type problem*, the conditional Bayes risk can be alternatively defined and evaluated by utilizing probabilities of the discrete states (d_0: undamaged, and d_1: damaged), such that

$$\begin{aligned} R_z(d_0; x_z) &= P_{D|X_z}(d_0|\text{sensor data } x_z)\alpha_{\min} \\ &\quad + P_{D|X_z}(d_1|\text{sensor data } x_z)\alpha_{\max}; \\ R_z(d_1; x_z) &= P_{D|X_z}(d_0|\text{sensor data } x_z)\beta_{\min} \\ &\quad + P_{D|X_z}(d_1|\text{sensor data } x_z)\beta_{\max}, \end{aligned} \tag{17}$$

from which the optimal decision may then be obtained as

$$\hat{d}_z = \underset{d_i}{\operatorname{argmin}}\, R_z(d_i; x_z). \tag{18}$$

There are several limitations and challenges with this traditional approach, especially for the structural health monitoring type of decision making where the structural state is continuously evolving with time. Such challenges include:

1. It is natural to define the structural state or the damage intensity as a continuous quantity, whereas, maintenance actions

(and their labels acting as a proxy discrete damaged state) are discrete. The decision-making framework proposed in this paper utilizes continuous damage intensity (or the state parameter) to make a maintenance decision. On the other hand, the decision-making approach using Eq. (17) and (18) requires objectively defining discrete damaged states d_i (unlike in the proposed approach, these discrete states are linked to the maintenance strategies). In a real-world problem, it is difficult to objectively define the discrete state of the structure since the structural state is continuous by its very nature. Secondly, any attempt to objectively define a discrete structural state is bound to be in terms of the continuous state parameter.

2. The current approach *directly/explicitly* utilizes the probability distribution of the state parameter to make a decision. On the other hand, the traditional approach utilizes the state parameter *implicitly* to make a decision. This is because the traditional approach requires establishing a classifier/detector (via a hypothesis test) to evaluate the probability of the discrete damage state conditioned on the probability distribution of the state parameter, which in turn is conditioned upon the strain measurements. Defining the classifiers (or a detector criterion) objectively requires a large amount of data (more specifically, features) that span the target damage states of interest, and supervised learning may be employed to define the classifiers. In the case of the SHM system installed on a complex structure with numerous sensors and an uncertain continuous degree of damage, such objective well-defined classifiers may not necessarily be obtainable. This is because, in practice, features are very unlikely to be obtained in all possible classification states (especially higher damage or failed states).
3. The expression of the expected cost evaluated using Eq. (17) and (18) (the traditional approach) is not an optimal form to incorporate behavioral biases in engineering decision-making. The approach that we have proposed was inherently designed to incorporate the behavioral psychology of the decision-maker all the while using the continuous nature of the structural state.

We deviate from the traditional approach used in detection/classification types of problems, where it is possible to objectively define the discrete classes and classifiers (equivalent to discrete structural states in SHM-based problems). Defining the classifiers objectively requires a large amount of data that spans the target classes (or damage states). However, unlike a well-defined detection type problem, objectively defining a mutually exclusive and exhaustive set of discrete structural states is challenging due to the lack of data and the complexity of the problem. In turn, we solve this problem by utilizing a damaged label associated with a maintenance strategy as a proxy to the discrete structural state.

Remark 2. We have assumed a linear form of the base costs $L(d_i, \theta_{\text{true}})$ for $i \in \{0, 1\}$ since this functional form satisfies monotonically increasing property and only requires knowledge of extreme costs which can reasonably estimated. In most cases, the consequence costs are reasonably obtained by estimating the current real cost of performing maintenance and by investigating the damage evolution model using the finite element model. As explained before, one noteworthy characteristic of the consequence cost is that it must be a non-decreasing function of the true damage intensity. When it comes to maintenance decisions guided by the organization's policies or collective experience, we consider the real-world scenario where inspection engineers are authorized to execute those decisions. These decisions are subjective to the engineer's experience and their thought processes but are assumed commensurate with the broader policies or guidance provided by the organization. Therefore, the *perceived* consequence weights of performing maintenance may deviate from the base consequence cost recommended by the organization, subject to engineering judgment. For example, engineers who know that there are some approximations in the base cost curves may want to make a more conservative maintenance decision (doing a bit more than what is required by the maintenance guide issued by the organization). The approximate nature of the base cost functions, and hence the underlying uncertainty in the cost, promote the inspection engineer to display *risk-aversion* [45]. Another situation that demands a deviation from the base cost functions is if the SHM system under-predicts or over-predicts the degree of damage (or the state parameter), causing the engineer to be either *risk-averse* or *risk-seeking*. Therefore, the base consequence functions can be modified to include risk intensity considered in the decision-making process. Recognizing that this risk perception of the decision-makers leads to modification of the base cost curve (to include desirable risk intensity), the organization can offer a spectrum of cost functions that can be chosen based on the desirable risk intensity of the decision-making process. The next section explores and models the risk profiles of the engineers. Empowered with the idea of the risk profiles, we will propose a spectrum of risk profiles that can be interpreted in two ways: (1) *forward interpretation*: each risk profile represents an individual decision-maker's behavior; (2) *inverse interpretation*: each risk profile represents a risk-intensity that the organization wants to include over the base cost to make a decision. A risk-averse profile demands a conservative decision, i.e., a tendency to perform the maintenance M_1 at a relatively lower level of damage to avoid any disastrous and expensive consequence. On the other hand, a risk-seeker profile allows more flexible decision-making that would recommend the maintenance M_1 only when the degree of structural damage is approaching failure, i.e., in a higher state of perceived risk.

4.3. Behavioral psychology and risk profiles

Decision-making under uncertainty is fundamental, and every decision involves consequence(s) associated with it; thus, it is expected that decision outcomes change from one individual to another based on how they perceive the consequences of making that decision. This is primarily due to biases and heuristics. The tendencies that govern our day-to-day decision-making are the very same behavioral tendencies that make maintenance decisions subjective to the engineer in charge. We demonstrate this fact by a simple example of *representative bias*. Irrespective of the true structural damage, the inspection engineers tend to delay the maintenance of the structure that does not show a sign of damage, and they are prompted to repair it when there is a visible form of damage. This is because the undamaged state of the structure *appears* safe (irrespective of the true structural state).

Another behavioral tendency of humans is that they inherently aim at maximizing rewards and minimizing losses. However, losing hurts more than winning brings joy. This concept of loss-aversion was first identified by Amos Tversky and Daniel Kahneman [42] as a critique of the expected utility theory which assumes that a rational decision-maker would weigh losses and wins equally when their absolute values are the same. They noted that people underweight outcomes that are merely probable in comparison with outcomes that are obtained with certainty, called the *certainty effect*. As a consequence of the certainty effect, they argued that decision-maker acts risk-aversely in a situation when decision choices involve sure gain and are happier with smaller certain gains than with larger probable gains; on the other hand, people exhibit risk-seeker behavior when the decision choices involve certain losses and are happier to bet on a larger but probable loss than a smaller but certain loss. This observation that risk aversion in the positive domains is accompanied by risk-seeking in the negative domain is called the *reflection effect*. As a consequence of the reflection effect, Tversky and Kahneman argued that we do not necessarily desire certainty, rather we " desire to lose less" more than we "desire to win", i.e., the certainty (or less uncertainty) increases the aversiveness of losses, as well as the desirability of gains. Charles Krauthammer (refer to chapter 3, pages 63–65 of [73]) wrote about loss-aversion in sports,

called the Krauthammer Conjecture, and noted: "*in sports, the pleasure of winning is less than the pain of losing*". He supported his claim by examples, including *"When the Cleveland Cavaliers lost the 2015 NBA Finals to Golden State, LeBron James sat motionless in the locker room, staring straight ahead, still wearing his game jersey, for 45 min after the final buzzer"*. Although humans are loss-averse, under uncertain situations a decision-maker needs to accept a risk and possible losses with an expectation of a reward.

It is these behavioral-psychological tendencies discussed above that lead different inspection engineers to have different expectations and intuitive/heuristic risk perception or knowledge of the possible consequence of making a decision or choosing the maintenance action, especially for the non-extreme values of the true degree of damage. The perceived importance of the outcome of making a decision is subjective to the individual. In general terms, an *individual's risk profile* is his/her willingness and ability to take risks and bear losses as a consequence of making a decision. A risk can be thought of as an acceptable loss that the individual is prepared to take for some expected return. For further discussion, we consider monetary losses. As such, risk profiles can be classified into *risk-aversion*, *risk-seeking*, and *risk-neutral*. A risk-averter decision-maker has a strong desire to not make any incorrect decisions that can lead to large losses. On the contrary, a risk-seeker is willing to bet more and absorb high losses with an expectation of the highest possible return. In short, a risk-averter decision-maker tends to make a safer/conservative decision settling for a moderate reward, whereas, a risk-seeker tends to risk larger losses expecting a bigger reward. However, we note that the willingness and the ability of a decision-maker to take risks need not necessarily match up. For instance, an entrepreneur with the same net worth as a lottery winner may have an equal *ability*, or capacity, to take a risk. Being fully aware of the uncertainties, however, an entrepreneur might be more *willing* to bet on new potential business than the lottery winner.

The risk profile of the decision-maker can be mathematically modeled by their utility vs. wealth (or loss) function, or generally a *utility function*. An individual's utility gives their evaluation of the consequence/outcome of an action. The utility may be different from the real dollar cost (or value). Since a risk-averse decision-maker aims at losing less (or gaining more), his/her perceived value of cost/loss is higher than the real dollar cost. This leads to an increasing concave-down utility function. On the other hand, a risk-seeker decision-maker is willing to risk more and hence assign a lower valuation to the real cost, leading to an increasing concave-up utility function. The readers are recommended to read the third essay in [74] titled: *"The theory of risk-aversion"*, which discusses the concept of risk aversion applied to the area of investment, insurance, risk-sharing, and liquidity demand behavior; and read Bernstein [75] for the history of risk and to understand the role of risk in our society.

The consequence of rating the structure as d_0 leads to consequence cost $L(d_0, \theta_{\text{true}})$ that ranges from $\alpha_{\min}$ to $\alpha_{\max}$. Similarly, rating the structure as d_1 leads to consequence cost $L(d_1, \theta_{\text{true}})$ that ranges from $\beta_{\min}$ to $\beta_{\max}$. Let $l_0 \in [\alpha_{\min}, \alpha_{\max}]$ and $l_1 \in [\beta_{\min}, \beta_{\max}]$ represent possible values of the consequence cost functions $L(d_0, \theta_{\text{true}})$ and $L(d_1, \theta_{\text{true}})$, respectively. We now define two utility functions $U(d_0, l_0)$ and $U(d_1, l_1)$ for decisions d_0 and d_1, respectively. To do so, we assume the following:

1. We assume that utility equals consequence cost at the extreme values of l_0 and l_1. That is, $U(d_0, \alpha_{\min}) = \alpha_{\min}$, $U(d_0, \alpha_{\max}) = \alpha_{\max}$, $U(d_1, \beta_{\min}) = \beta_{\min}$ and $U(d_1, \beta_{\max}) = \beta_{\max}$. This is because these costs represent extreme damage scenarios and are assumed to be fixed by the organization. It is a valid assumption since different individuals can agree with the consequence-cost decided by the organization at extreme values of the gap length. It is this constraint that requires definition of two different utility functions for the decisions d_0 and d_1, respectively.
2. To model the aforementioned utility functions, we define the *critical losses* $l_{c0} \in [\alpha_{\min}, \alpha_{\max}]$ and $l_{c1} \in [\beta_{\min}, \beta_{\max}]$ as consequence costs at which utilities are defined as $U(d_0, l_{c0}) = \gamma\alpha_{\max} + (1-\gamma)\alpha_{\min}$, and $U(d_1, l_{c1}) = \gamma\beta_{\max} + (1-\gamma)\beta_{\min}$ for labeling scenarios d_0, and d_1, respectively. Here, $\gamma \in [0, 1]$ represents the fractional distance between extreme costs $[\alpha_{\min}, \alpha_{\max}]$ or $[\beta_{\min}, \beta_{\max}]$ and it satisfies the conditions above. It is one of the two quantities that parameterize the utility function. It must be reasonably chosen to be used for a desirable utility function. Therefore, a unique pair of (l_{c0}, γ) and (l_{c1}, γ) yields a unique set of utility functions $U(d_0, l_0)$ and $U(d_1, l_1)$, respectively. We assume these utility functions to bear the following form

$$\begin{aligned} U(d_0, l_0) &= a_0 \log((l_0 - \alpha_{\min})b_0 + 1) + \alpha_{\min}; \\ U(d_1, l_1) &= a_1 \log((l_1 - \beta_{\min})b_1 + 1) + \beta_{\min}. \end{aligned} \tag{19}$$

The constants a_0 and b_0 are obtained by using the definition of the *critical losses* and solving the following simultaneous non-linear equations:

$$\begin{aligned} a_0 \log\left((\alpha_{\max} - \alpha_{\min})b_0 + 1\right) &= U(d_0, \alpha_{\max}) - U(d_0, \alpha_{\min}) \\ &= \alpha_{\max} - \alpha_{\min}; \\ a_0 \log\left((l_{c0} - \alpha_{\min})b_0 + 1\right) &= \gamma(U(d_0, \alpha_{\max}) - U(d_0, \alpha_{\min})) \\ &= \gamma(\alpha_{\max} - \alpha_{\min}). \end{aligned} \tag{20}$$

Similarly, the constants a_1 and b_1 can be obtained by solving the following equations:

$$\begin{aligned} a_1 \log\left((\beta_{\max} - \beta_{\min})b_1 + 1\right) &= U(d_1, \beta_{\max}) - U(d_1, \beta_{\min}) \\ &= \beta_{\max} - \beta_{\min}; \\ a_1 \log\left((l_{c1} - \beta_{\min})b_1 + 1\right) &= \gamma(U(d_1, \beta_{\max}) - U(d_1, \beta_{\min})) \\ &= \gamma(\beta_{\max} - \beta_{\min}). \end{aligned} \tag{21}$$

Eqs. (20) and (21) are not solvable for $l_{c0} = \gamma\alpha_{\max} + (1-\gamma)\alpha_{\min}$ and $l_{c1} = \gamma\beta_{\max} + (1-\gamma)\beta_{\min}$ respectively. However, as $l_{c0} \longrightarrow (\gamma\alpha_{\max} + (1-\gamma)\alpha_{\min})$ and $l_{c1} \longrightarrow (\gamma\beta_{\max} + (1-\gamma)\beta_{\min})$, the utility function (or equivalently the risk-profile) looses its curvature and becomes linear, i.e, the utility reduces to the value (or dollar cost), i.e, $U(d_0, l_0) = l_0$ and $U(d_1, l_1) = l_1$. This reflects a *risk-neutral* behavior. Therefore, the three cases of risk profile can then be classified by the following:

$$\begin{aligned} &l_{c0} < \gamma\alpha_{\max} + (1-\gamma)\alpha_{\min} \text{ and } l_{c1} < \gamma\beta_{\max} + (1-\gamma)\beta_{\min} : \text{ Risk-aversion;} \\ &l_{c0} = \gamma\alpha_{\max} + (1-\gamma)\alpha_{\min} \text{ and } l_{c1} = \gamma\beta_{\max} + (1-\gamma)\beta_{\min} : \text{ Risk-neutral;} \\ &l_{c0} > \gamma\alpha_{\max} + (1-\gamma)\alpha_{\min} \text{ and } l_{c1} > \gamma\beta_{\max} + (1-\gamma)\beta_{\min} : \text{ Risk-seeking.} \end{aligned} \tag{22}$$

Although we have two different utility functions for decisions d_0 and d_1, respectively, for a given triad (γ, l_{c0}, l_{1c}), an individual with his/her unique risk perception should have a unique relationship between their utility functions. To define a unique set of utility functions for a given individual (or for a unique risk intensity), we establish a relationship between the critical costs l_{c0} and l_{c1}

$$\xi = \frac{l_{c0} - \alpha_{\min}}{\alpha_{\max} - \alpha_{\min}} = \frac{l_{c1} - \beta_{\min}}{\beta_{\max} - \beta_{\min}}. \tag{23}$$

Here, $\xi \in [0, 1]$ is the *critical fractional distance*. The constraint in Eq. (23) and the following definition of the *critical fractional distance* ξ allows us to uniquely parameterize a risk profile by two non-dimensional and normalized parameters (γ, ξ) yielding a set of two unique utility functions. From here on, we denote the utilities $U(d_0, l_0)$ and $U(d_1, l_1)$ as $U(d_0, l_0; \gamma, \xi)$ and $U(d_1, l_1; \gamma, \xi)$, respectively, where the parameters (γ, ξ) characterizes the risk-profile. Based on the discussion above and Eq. (22), the three cases of risk profile are classified as follows:

$$\begin{aligned} &\xi < \gamma : \text{ Risk-averter;} \\ &\xi = \gamma : \text{ Risk-neutral;} \\ &\xi > \gamma : \text{ Risk-seeker.} \end{aligned} \tag{24}$$

Table 2
Examples of different risk profiles.

Risk profiles	ID	γ	ξ	Critical loss l_{c0}	Critical loss l_{c1}
				Critical losses l_{c0} and l_{c1} are related by Eq. (23)	
Extreme risk-averter	RP1	0.8	0.25	$l_{c0} = 0.25\alpha_{\max} + 0.75\alpha_{\min}$	$l_{c1} = 0.25\beta_{\max} + 0.75\beta_{\min}$
Moderate risk-averter	RP2	0.8	0.6	$l_{c0} = 0.6\alpha_{\max} + 0.4\alpha_{\min}$	$l_{c1} = 0.6\beta_{\max} + 0.4\beta_{\min}$
Neutral risk bearer	RP3	0.8	0.8	$l_{c0} \longrightarrow \gamma\alpha_{\max} + (1-\gamma)\alpha_{\min}$	$l_{c1} \longrightarrow \gamma\beta_{\max} + (1-\gamma)\beta_{\min}$
Moderate risk-seeker	RP4	0.8	0.95	$l_{c0} = 0.95\alpha_{\max} + 0.05\alpha_{\min}$	$l_{c1} = 0.95\beta_{\max} + 0.05\beta_{\min}$
Extreme risk-seeker	RP5	0.8	0.999	$l_{c0} = 0.999\alpha_{\max} + 0.001\alpha_{\min}$	$l_{c1} = 0.999\beta_{\max} + 0.001\beta_{\min}$

We have two other extreme cases. When $l_{c0} \longrightarrow \alpha_{\min}$ and $l_{c1} \longrightarrow \beta_{\min}$, it limits the constants $b_0 \longrightarrow \infty$ and $b_1 \longrightarrow \infty$, respectively, representing the *extreme risk-averse* behavior with *asymptotic concave-down* utility function. Similarly, when $l_{c0} \longrightarrow \alpha_{\max}$ and $l_{c1} \longrightarrow \beta_{\max}$, it constraints the constants $b_0 \longrightarrow 1$ and $b_1 \longrightarrow 1$, respectively, representing the *extreme risk-seeker* behavior with *asymptotic concave-up* utility function. The behavior of every individual with a unique risk intensity is characterized by two utility functions $U(d_0, l_0; \gamma, \xi)$ (plotted in Fig. 4(a)) and $U(d_1, l_1; \gamma, \xi)$ (plotted in Fig. 4(b)) bound by the constraint in Eq. (23). Using the utility functions plotted in Figs. 4(a) and 4(b), we define 5 risk profiles (RP) obtained using $\gamma = 0.8$ (reasonably assumed) and ξ spanning from 0 to 1 in Table 2. These risk profiles will later be used in numerical simulations.

We justify the functional form of utility function modeled by Eq. (19) by noting the following properties of the utility $U(d_0, l_0; \gamma, \xi)$ (same arguments hold for the utility $U(d_1, l_1; \gamma, \xi)$):

1. The utility function of form $U(d_0, l_0; \gamma, \xi) = a_0 \log((l_0 - \alpha_{\min})b_0 + 1) + \alpha_{\min}$ satisfies one of the primary tenet of expected utility theory as defined in [42], which is: all the concave-down utility function curves with $\left(\partial^2_{l_0} U(d_0, l_0; \gamma, \xi) < 0\right)$ represent a risk-averse behavior, whereas, the concave-up curves with $\left(\partial^2_{l_0} U(d_0, l_0; \gamma, \xi) > 0\right)$ represent a risk-seeker. This is clearly illustrated in Figs. 4(c) and 4(d) for the utilities $U(d_0, l_0; \gamma, \xi)$ and $U(d_1, l_1; \gamma, \xi)$, respectively.
2. Pratt [76] noted that the *local risk intensity* factor, defined by $-\left(\frac{\partial^2_{l_0} U(d_0, l_0; \gamma, \xi)}{\partial_{l_0} U(d_0, l_0; \gamma, \xi)}\right)$, is the correct measure of the local intensity of the risk behavior. For two risk-averse profiles $U_a(d_0, l_0; \gamma, \xi)$, and $U_b(d_0, l_0; \gamma, \xi)$, if $-\left(\frac{\partial^2_{l_0} U_a(d_0, l_0; \gamma, \xi)}{\partial_{l_0} U_a(d_0, l_0; \gamma, \xi)}\right) > -\left(\frac{\partial^2_{l_0} U_b(d_0, l_0; \gamma, \xi)}{\partial_{l_0} U_b(d_0, l_0 \gamma, \xi)}\right)$, then $U_a(d_0, l_0; \gamma, \xi)$ is locally more risk-averse than $U_b(d_0, l_0; \gamma, \xi)$. On the other hand, for two risk-seeker profiles $U_a(d_0, l_0; \gamma, \xi)$, and $U_b(d_0, l_0; \gamma, \xi)$, if $-\left(\frac{\partial^2_{l_0} U_a(d_0, l_0; \gamma, \xi)}{\partial_{l_0} U_a(d_0, l_0; \gamma, \xi)}\right) < -\left(\frac{\partial^2_{l_0} U_b(d_0, l_0; \gamma, \xi)}{\partial_{l_0} U_b(d_0, l_0; \gamma, \xi)}\right)$, then $U_a(d_0, l_0; \gamma, \xi)$ is locally more risk-seeker than $U_b(d_0, l_0; \gamma, \xi)$. We also note that the vanishing local risk intensity factor $-\left(\frac{\partial^2_{l_0} U(d_0, l_0; \gamma, \xi)}{\partial_{l_0} U(d_0, l_0; \gamma, \xi)}\right) = 0$ implies constant risk, for which, the cost function is linear. The form of utility function used in this paper clearly exhibits the discussed properties for all values of the loss as seen in Figs. 4(e) and 4(f) for the utilities $U(d_0, l_0; \gamma, \xi)$ and $U(d_1, l_1; \gamma, \xi)$, respectively.

Markowitz [71] noted the possibility that the utility function may have both concave and convex regions for the scenarios involving both gains and losses. We cautiously note that, in this paper, we did not account for such cases where a decision-maker exhibits varying risk behavior at different values of the gap length. Apart from the risk profile, the discussion and approaches for decision-making remain the same.

An organization like USACE consists of numerous maintenance action decision-makers and policymakers who share a spectrum of risk profiles. Every single action by any employee of an organization affects the collective performance of an organization. As discussed in [37], although difficult to precisely define, an organization has a risk profile based on its alignment with values and priorities. Assuming that an organization is as good as its employees in an average sense, we propose that the *organizational risk profile* be defined based on the weighted average consequences of the decisions made by the employees, which in turn depends on the distribution of the risk-intensities of individual decision-makers. We refer to the distribution of various risk profiles of decision-makers employed by the organization as the *organizational risk profile* (ORP). Methodology to psychologically evaluate and define an individual's risk profile is beyond the scope of this paper. However, one approach to infer the individual risk profile is by analyzing their past actions and by designing a set of questionnaires (as is very common in the field of behavioral economics) with a goal of extracting their risk profiles.

We provide a simple example of the risk profile of *collective decision makers*. Just like any organization, the performance of the stock market (quantified by the S&P500 index, for example) is governed by millions of participants (speculators and investors) who have different risk profiles. At an individual level, the risk profile of an investor is a direct function of their age, investing skill, and experience in investing. Additionally, analogous to how organizational values and goals also impact the risk profiles of the engineers/managers, the current risk profile of the market also influences the behavior of its participants. Investor George Soros calls this feedback loop of risk behavior of the participants influencing the market, and the market conditions influencing the behavior of the participants, as *the Principle of Reflexivity* [77]. In the bull market, there are more investors betting on a growing economy and higher S&P500 prices. As the price of the S&P500 goes up, the risk of major correction increases — that is, the market becomes a "risk-seeker". In the bear market, there are more sellers than buyers of equities, which leads the price of S&P500 to go down, which in turn reduces the overall risk of investments — that is, the market becomes "risk-averse".

In this paper, we focus our attention on investigating the collective performance of an organization by considering two different *organizational risk profiles*–ORP1 and ORP2, detailed later in this section. Recall that for the miter gate problem, the risk-profile of the decision-maker is parameterized by two parameters (γ, ξ) and depends on the extreme costs $\alpha_{\min}$, $\alpha_{\max}$, $\beta_{\min}$, and $\beta_{\max}$. Hence, for a fixed value of γ, and the extreme costs $\alpha_{\min}$, $\alpha_{\max}$ (normalized to be unity), $\beta_{\min}$, and $\beta_{\max}$, the risk profile is uniquely parameterized by ξ. For such a case, the *organizational risk profile* (here USACE) can be quantified by the distribution of $\xi \in \Omega_\Xi$, denoted by $f_\Xi(\xi)$. For the purpose of demonstration, we assume that the risk profiles of the decision-makers at USACE range from *Moderate Risk Aversion* to *Moderate Risk Seeking*. Recall from Table 2, for a fixed $\gamma = 0.8$, the value of ξ in the neighborhood of 0.6 defines *Moderate Risk Averse* profile, and ξ in the neighborhood of 0.95 defines Moderate risk-seeker profile. Thus, we assume that the decision-makers at USACE have risk profiles ranging from $(\gamma = 0.8, \xi = 0.55)$ to $(\gamma = 0.8, \xi = 0.975)$, i.e., $\Omega_\Xi = [0.55, 0.975]$. With these bounds on the risk profiles of the decision-makers, we assume two organizational risk profiles (ORP1 and ORP2) as illustrated in Fig. 5. Since a higher value of ξ implies more risk-seeker behavior,

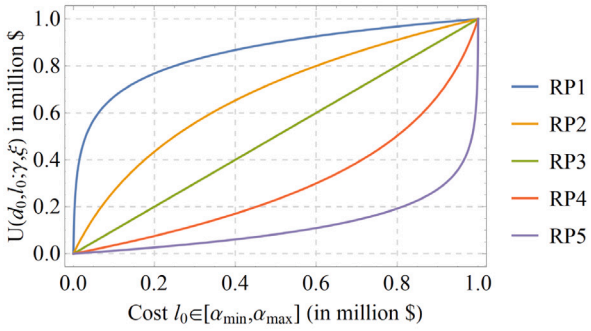

(a) Utility function $U(d_0, l_0; \gamma, \xi)$

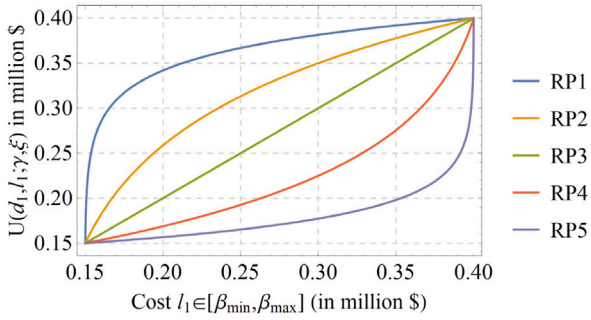

(b) Utility function $U(d_1, l_1; \gamma, \xi)$

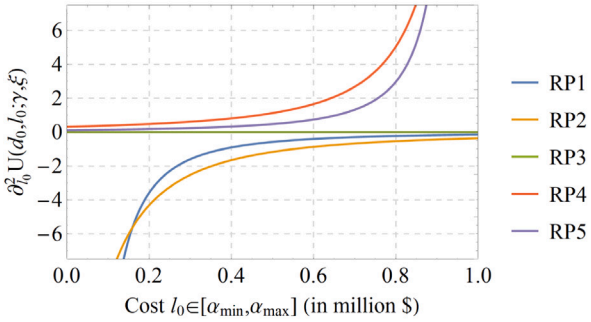

(c) Second derivative of utility function $U(d_0, l_0; \gamma, \xi)$

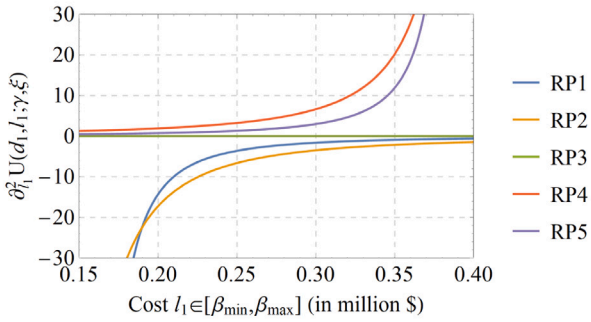

(d) Second derivative of utility function $U(d_1, l_1; \gamma, \xi)$

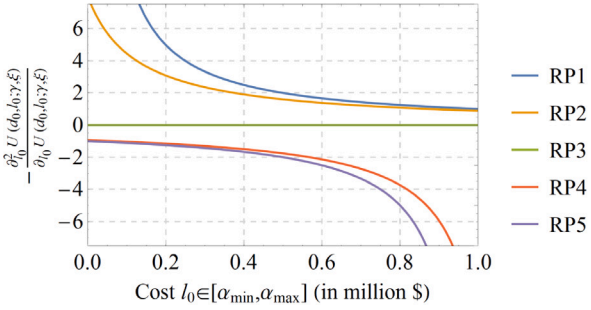

(e) Local risk intensity factor of utility function $U(d_0, l_0; \gamma, \xi)$

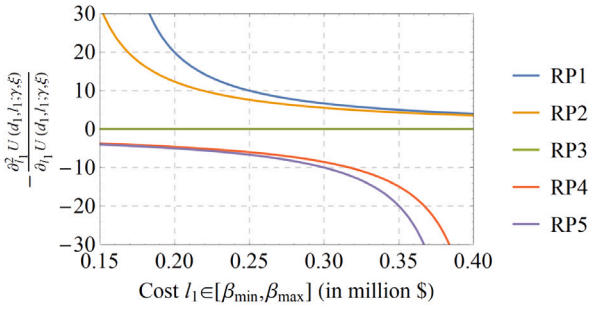

(f) Local risk intensity factor of utility function $U(d_1, l_1; \gamma, \xi)$

Fig. 4. Risk profiles modeled by utility vs. loss, or simply utility function assuming $\gamma = 0.8$ and ξ defined in Table 2.

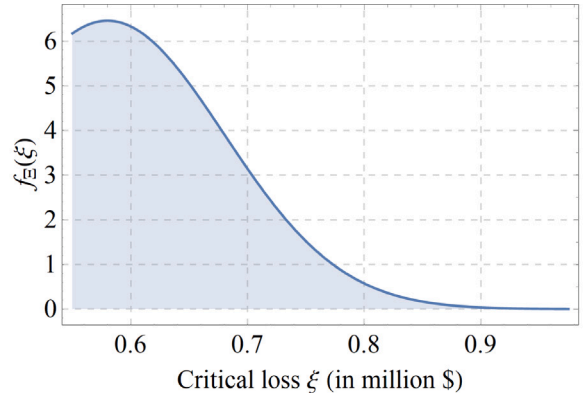

(a) Risk-averse organizational risk profile (ORP1)

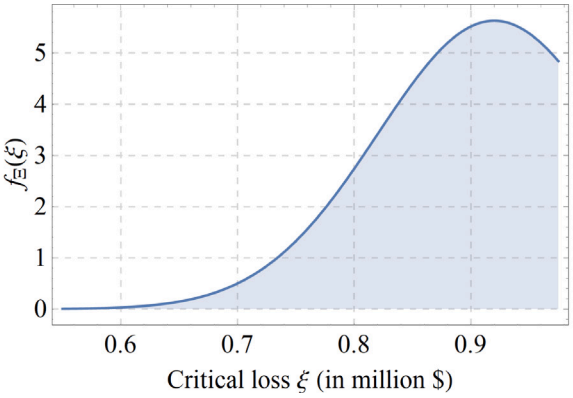

(b) Risk-seeker organizational risk profile (ORP2)

Fig. 5. Organizational risk behavior as defined by $f_{\Xi}(\xi)$.

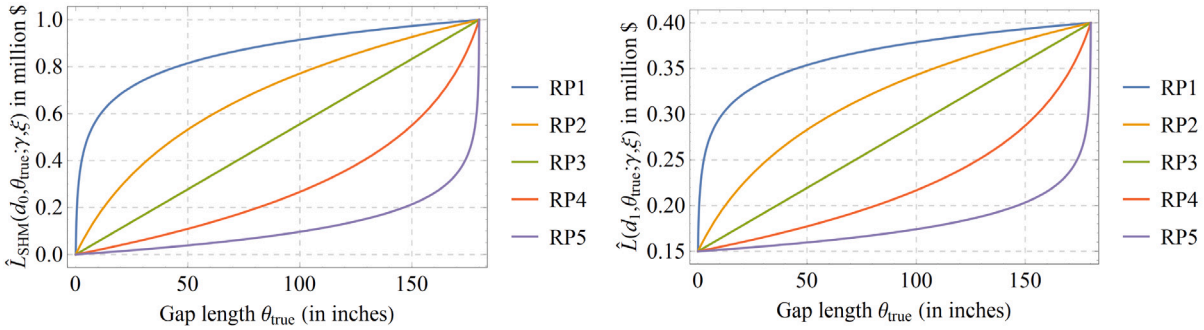

(a) Modified cost function for label d_0 (b) Modified cost function for label d_1

Fig. 6. Risk intensity modified cost function.

ORP1 represents a more risk-averse behavior than ORP2. In Section 5, we simulate and investigate the impact of individual risk profiles (RP1 to RP5), and the organizational risk profiles (ORP1 and ORP2) on decision making.

4.4. Risk intensity modified cost functions

Since perceived value of a loss depends on individual's utility (or the risk-perception, or the specified risk-intensity), we can obtain the *modified consequence-costs* of performing maintenance strategies M_0 and M_1, respectively, by substituting the losses l_0 and l_1 (arguments in the utility function defined in Eq. (19)) by the consequence-cost $L(d_0,\theta_{true})$ and $L(d_1,\theta_{true})$ defined in Eq. (16), respectively. We denote $\hat{L}(d_0,\theta_{true};\gamma,\xi)$ and $\hat{L}(d_1,\theta_{true};\gamma,\xi)$ (distinguished by a hat $\hat{(\cdot)}$) as the *modified consequence-costs* of performing maintenance strategies M_0 and M_1 respectively. This allows us to incorporate the risk-perception into the decision making process. Using Eqs. (16) and (19), we get

$$\begin{aligned}\hat{L}(d_0,\theta_{true};\gamma,\xi) &= U(d_0, L(d_0,\theta_{true});\gamma,\xi)\\ &= a_0 \log\left(1 + b_0\left(\frac{\alpha_{max}-\alpha_{min}}{\theta_{max}-\theta_{min}}\right)\theta_{true}\right) + \alpha_{min};\\ \hat{L}(d_1,\theta_{true};\gamma,\xi) &= U(d_1, L(d_1,\theta_{true});\gamma,\xi)\\ &= a_1 \log\left(1 + b_1\left(\frac{\beta_{max}-\beta_{min}}{\theta_{max}-\theta_{min}}\right)\theta_{true}\right) + \beta_{min}.\end{aligned} \tag{25}$$

For a given risk profile (γ,ξ), the constants a_0, a_1, b_0, and b_1 are obtained by solving Eqs. (20) and (21). Fig. 6 plots the modified cost functions for the various risk profiles defined in Table 2. We note that

$$\begin{aligned}&\hat{L}(d_i,\theta_{true};\gamma,\xi) > L(d_i,\theta_{true}) : \text{ for risk-averse profile;}\\ &\hat{L}(d_i,\theta_{true};\gamma,\xi) = L(d_i,\theta_{true}) : \text{ for risk-neutral profile;}\\ &\hat{L}(d_i,\theta_{true};\gamma,\xi) < L(d_i,\theta_{true}) : \text{ for risk-seeker profile.}\end{aligned} \tag{26}$$

Unlike classification-type problems in supervised machine learning, in this case, it is not possible to define a unique classifier for deciding whether the structure should be labeled damaged or undamaged. This is because decision-making is subjective in the current scenario, and it depends on two sources of information: the posterior distribution of the gap length (the damage parameter) θ and the risk profile of the engineer/decision-maker. To quantify and model the intensity of the risk behavior, we attempt to uniquely define a classifier for a special case where the true value of the gap length is measurable (obtained by performing a perfect experiment). Under this situation, when θ_{true} can be accurately and deterministically inferred, we define a classifier threshold $\tilde{\theta} \in \Omega_\Theta$ as the gap length at which the consequence costs of performing M_0 and M_1 are equal, i.e.,

$$\begin{aligned}&\theta_{true} < \tilde{\theta} : \text{ Perform } M_0;\\ &\theta_{true} > \tilde{\theta} : \text{ Perform } M_1,\end{aligned} \tag{27}$$

where the classifier $\tilde{\theta}$ satisfies the following:

$$\begin{aligned}&\text{When risk-intensity is not included} : L(d_0,\tilde{\theta}) = L(d_1,\tilde{\theta});\\ &\text{When risk-intensity is included} : \hat{L}(d_0,\tilde{\theta};\gamma,\xi) = \hat{L}(d_1,\tilde{\theta};\gamma,\xi).\end{aligned} \tag{28}$$

Larger the value of $\tilde{\theta}$, higher the intensity of risk-seeker behavior and vice versa. Table 3 gives the classifier $\tilde{\theta}$ for various risk profiles. It is obvious that among the risk profiles considered in Table 2, RP5 represents the most intense risk-seeker behavior, whereas RP1 represents the most intense risk-averse behavior. This can also be seen in Fig. 7. Figs. 7(a) and 7(b) compare the classifier for risk-averse (RP2) and risk-seeker (RP4) profiles relative to a risk-neutral profile (RP3).

Remark 3. In the approach presented, we assume that any two decision-makers agree upon the prior probability distribution of gap length, agree upon modeling the likelihood function using a Gaussian distribution, and agree on the consequence costs at extreme values of θ_{true}. We only model risk preferences of individuals at non-extreme values of θ_{true} through utility functions. Finally, we also assume that there are no measurement biases and that the noise in sensor measurements is random.

5. Prior and posterior decision analysis

To acquire new information in support of decision making, we assume that an SHM system z is installed, as is the case with the USACE miter gate shown in Fig. 2. Since the system is already installed, this is a posterior decision analysis and not a preposterior analysis. Installing an SHM system incurs an intrinsic cost $C(z)$. We assume that intrinsic cost to be a fraction of the maximum cost α_{max}, i.e., $C(z) = 0.05\alpha_{max}$. The total cost function for an information-acquiring system z, denoted by $\hat{L}_z(d_i,\theta_{true};\gamma,\xi)$, is defined as the sum total of the extrinsic (for the various risk-profiles defined in Table 2) and the intrinsic cost-functions used for posterior decision analysis, wherein

$$\hat{L}_z(d_i,\theta_{true};\gamma,\xi) = C(z) + \hat{L}(d_i,\theta_{true};\gamma,\xi), \text{ for } i \in 0,1. \tag{29}$$

The cost function $\hat{L}_z(d_i,\theta_{true};\gamma,\xi)$ for various risk-profiles can be obtained by translating the curves in Fig. 6 upward of the value provided by $C(z)$. Given the following information:

1. The posterior probability distribution of the gap length $f_{\Theta|X_z}(\theta|x_z)$ obtained by Bayesian inference using new data acquired from the SHM system, and an updated finite element model discussed in Section 3.2;
2. The extrinsic cost as a consequence of making a decision $\hat{L}(d_i,\theta_{true};\gamma,\xi)$ discussed in Section 4.3; and
3. The intrinsic cost $C(z)$ of installing the SHM system,

the problem is to decide which maintenance strategy to perform–M_0 or M_1– or equivalently, what label/rating shall be assigned to the miter gate, d_0 or d_1.

Table 3
Classifier for various risk profiles.

Risk profile	RP1	RP2	RP3	RP4	RP5
Classifier $\tilde{\theta}$ (in inches) for $\gamma = 0.8$	0.533	12.421	35.999	81.392	146.323

Table 4
Various cases of the posterior probability distribution used in the posterior decision analysis.

Cases	Parameters of FE model for data simulation				σ_{strain} in Eq. (13) ($\times 10^{-6}$)	Posterior statistics		
	θ_{true} (in)	$h_{\text{up-true}}$ (in)	$h_{\text{down-true}}$ (in)	$\sigma_{\text{strain-true}}$ ($\times 10^{-6}$)		$\mu_{\theta\|x_z}$ (in)	$\sigma_{\theta\|x_z}$ (in)	$\rho_{\theta\|x_z} = \frac{\sigma_{\theta\|x_z}}{\mu_{\theta\|x_z}}$
Case 1	10.0	551.25	166.51	30	20	10.49	2.72	0.259
Case 2	50.0	560.53	185.06	50	60	44.68	13.02	0.290
Case 3	90.0	556.57	177.15	70	60	97.70	14.21	0.145
Case 4	130.0	543.07	150.14	90	70	140.78	11.25	0.0799
Case 5	170.0	542.59	149.18	100	70	158.78	11.38	0.0716

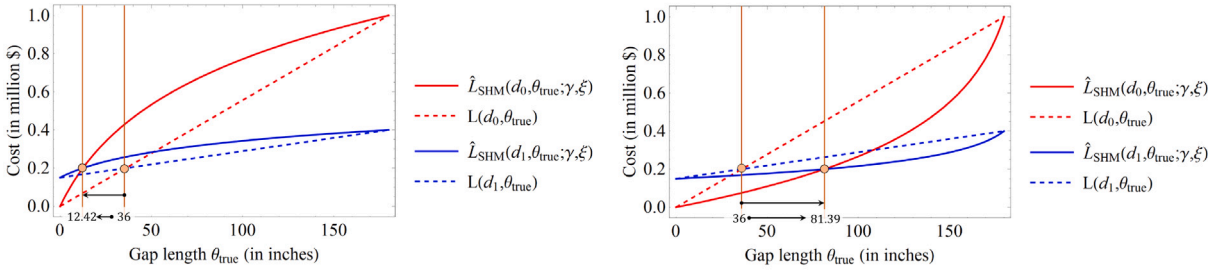

(a) Left-shift due to risk-averse behavior RP2 (b) Right-shift due to risk-seeker behavior RP4

Fig. 7. Shift in the classifier due to skewed risk-perception (here it is assumed that the data is acquired through an SHM system, i.e., $\hat{L}_z(\cdot) = \hat{L}_{\text{SHM}}(\cdot)$)

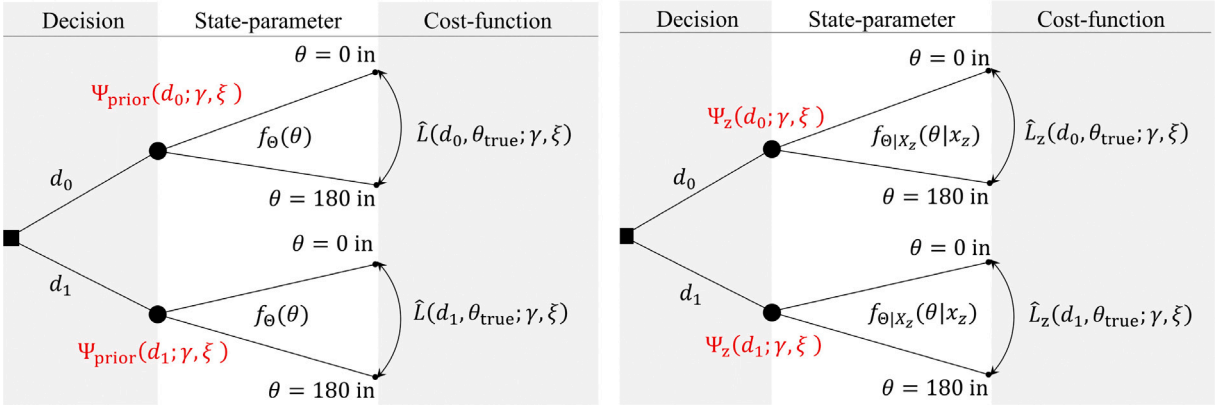

(a) Prior decision analysis (b) Posterior decision analysis

Fig. 8. Decision tree for prior and posterior decision analysis.

We start with a uniform prior distribution of the gap length representing a case where no additional information is acquirable, such that $f_\Theta(\theta) = (\theta_{\max} - \theta_{\min})^{-1}$. Recall here that we have assumed $\theta_{\min} = 0$ inches and $\theta_{\max} = 180$ inches. When prior analysis is performed, only the extrinsic risk-modified consequence cost $\hat{L}(d_i, \theta_{\text{true}}; \gamma, \xi)$ is used because the prior analysis assumes that no new information gathering mechanism is available. When the new information $x_z \in \Omega_{X_z}$ is obtained from the sensor array deployed on the miter gate, the posterior distribution of the gap length $f_{\Theta|X_z}(\theta|x_z)$ is obtained using Bayesian inference. In this case, the total cost $\hat{L}_z\left(d_i, \theta_{\text{true}}; \gamma, \xi\right)$ is considered. The optimal decision is then obtained as

$$\mathscr{A}_{\text{prior}}(\gamma,\xi) = \underset{d_i}{\operatorname{argmin}}\, \Psi_{\text{prior}}(d_i;\gamma,\xi) = \underset{d_i}{\operatorname{argmin}}\, E_\Theta\left[\hat{L}\left(d_i, \theta_{\text{true}} = \theta; \gamma, \xi\right)\right];$$
$$\mathscr{A}_z(\gamma,\xi) = \underset{d_i}{\operatorname{argmin}}\, \Psi_z(d_i;\gamma,\xi) = \underset{d_i}{\operatorname{argmin}}\, E_{\Theta|X_z}\left[\hat{L}_z\left(d_i, \theta_{\text{true}} = \theta; \gamma, \xi\right)\right]. \tag{30}$$

Here, $\mathscr{A}_{\text{prior}}(\gamma,\xi)$ and $\mathscr{A}_z(\gamma,\xi)$ denote optimal ratings arrived by using prior and posterior distribution of the gap length, respectively, for the risk-profile parameterized by (γ,ξ).

Figs. 8(a) and 8(b) illustrates the decision-tree for the prior and the posterior decision analysis, respectively. Following the traditional convention of decision trees, we denote the decision nodes by squares and the choices by circles.

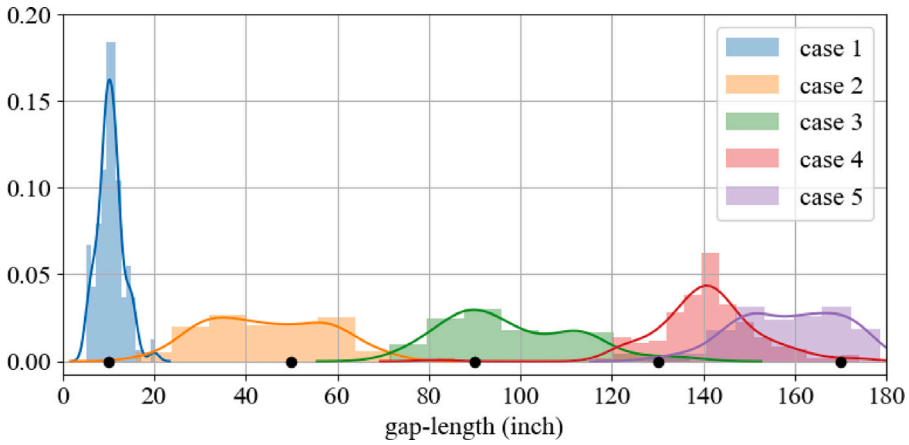

Fig. 9. Posterior probability distribution of gap length.

Table 5
The Bayes risk for different gap length distributions (cases 1–5) for decision d_0 (undamaged rating).

Cases		$\Psi_{\text{prior}}(d_0;\gamma,\xi)$ and $\Psi_z(d_0;\gamma,\xi)$ in million $				
		extreme risk-averter (RP1) $\tilde{\theta}=0.533$ in	Mild risk-averter (RP2) $\tilde{\theta}=12.421$ in	Neutral risk bearer (RP3) $\tilde{\theta}=35.999$ in	Mild risk-seeker (RP4) $\tilde{\theta}=81.392$ in	extreme risk-seeker (RP5) $\tilde{\theta}=146.323$ in
Posterior	Case 1	0.637	0.223	0.108	0.0704	0.0572
	Case 2	0.842	0.539	0.298	0.148	0.0846
	Case 3	0.960	0.810	0.592	0.312	0.145
	Case 4	1.014	0.951	0.832	0.538	0.238
	Case 5	1.032	0.999	0.932	0.708	0.329
Prior		0.910	0.727	0.557	0.350	0.170

Table 6
The Bayes risk for different gap length distributions (cases 1-5) for decision d_1 (damaged rating).

Cases		$\Psi_{\text{prior}}(d_1;\gamma,\xi)$ and $\Psi_z(d_1;\gamma,\xi)$ in million $				
		extreme risk-averter (RP1) $\tilde{\theta}=0.533$ in	Mild risk-averter (RP2) $\tilde{\theta}=12.421$ in	Neutral risk bearer (RP3) $\tilde{\theta}=35.999$ in	Mild risk-seeker (RP4) $\tilde{\theta}=81.392$ in	extreme risk-seeker (RP5) $\tilde{\theta}=146.323$ in
Posterior	Case 1	0.347	0.243	0.214	0.205	0.201
	Case 2	0.398	0.322	0.262	0.224	0.208
	Case 3	0.427	0.390	0.336	0.265	0.224
	Case 4	0.441	0.425	0.395	0.322	0.247
	Case 5	0.445	0.437	0.420	0.364	0.270
Prior		0.415	0.369	0.327	0.275	0.230

We parametrically investigate the sensitivity of risk perception on decision-making by considering the various risk profiles (RP) defined in Table 2. We consider five gap-length posterior distribution cases. Fig. 9 shows these posterior distributions of gap length with increasing mean values covering the entire domain of the gap length. It took approximately 20 h to obtain the posterior distribution in each case using an Intel Xeon W-2155 @ 3.30 GHz, 10 core, 128 GB memory workstation. Parallel computing was exploited to obtain the posterior distribution. The black dots in Fig. 9 indicate the true gap length θ_{true} which was used to simulate the strain data. Table 4 provides the parameters of the FE model for data simulation (i.e., true parameters), and reports the statistics of posterior distribution (mean $\mu_{\theta|x_z}$, standard-deviation $\sigma_{\theta|x_z}$, and coefficient of variation $\rho_{\theta|x_z}$). It also provides the standard deviation of the measurement noise that is considered in the inference. Observe that $\sigma_{\text{strain}} \neq \sigma_{\text{strain-true}}$, the reason for which is discussed at the end of Section 3.2.

Tables 5 and 6 present the results of prior and posterior analysis obtained using Eq. (30) for the risk profiles defined in Table 2. Table 7 shows the optimal decisions obtained for all the posterior distributions defined in Table 4 and all the risk profiles described in Table 2. From Tables 5, 6, and 7, we observe the following:

1. The extreme risk-averter (RP1) avoids making any risky decision and decides to perform maintenance M_1 (or label the structure d_1) for all the posterior cases (even for the case where the simulated true gap length value if $\theta_{\text{true}} = 10$ in). Considering the other extreme, the extreme risk-seeker (RP5) rates the gate as undamaged, or d_0, for all the posterior cases except for case 4 (with simulated $\theta_{\text{true}} = 130$ in) and case 5 (with simulated $\theta_{\text{true}} = 170$ in). We see that as the intensity of the risk-seeking behavior increases, or equivalently as the intensity of the risk-aversion behavior decreases, the cases with the rating d_0 increase. This is in line with the fact that the risk-seeker is willing to take his/her chances of making a false decision for the purpose of reducing the inspection or maintenance cost that follows with the decision d_1.
2. Cases 4 and 5 represent the situation when the gap length approaches its extreme value. As expected, as the value of gap length approaches the extreme value of $\theta_{\max}$, all the risk profiles decide that the gate is damaged (i.e., d_1).
3. In a real-world situation, the true value of gap length θ_{true} is not known. However, since we had simulated the posterior, we know

Table 7
The optimal decision for various risk profiles.

Cases		Optimal rating				
		extreme risk-averter (RP1) $\tilde{\theta} = 0.533$ in	Mild risk-averter (RP2) $\tilde{\theta} = 12.421$ in	Neutral risk bearer (RP3) $\tilde{\theta} = 35.999$ in	Mild risk-seeker (RP4) $\tilde{\theta} = 81.392$ in	extreme risk-seeker (RP5) $\tilde{\theta} = 146.323$ in
Posterior	Case 1 $\theta_{\text{true}} = 10$ in	d_1	d_0	d_0	d_0	d_0
	Case 2 $\theta_{\text{true}} = 50$ in	d_1	d_1	d_1	d_0	d_0
	Case 3 $\theta_{\text{true}} = 90$ in	d_1	d_1	d_1	d_1	d_0
	Case 4 $\theta_{\text{true}} = 130$ in	d_1	d_1	d_1	d_1	d_1
	Case 5 $\theta_{\text{true}} = 170$ in	d_1	d_1	d_1	d_1	d_1
Prior $\mu_\theta = 90$ in		d_1	d_1	d_1	d_1	d_0

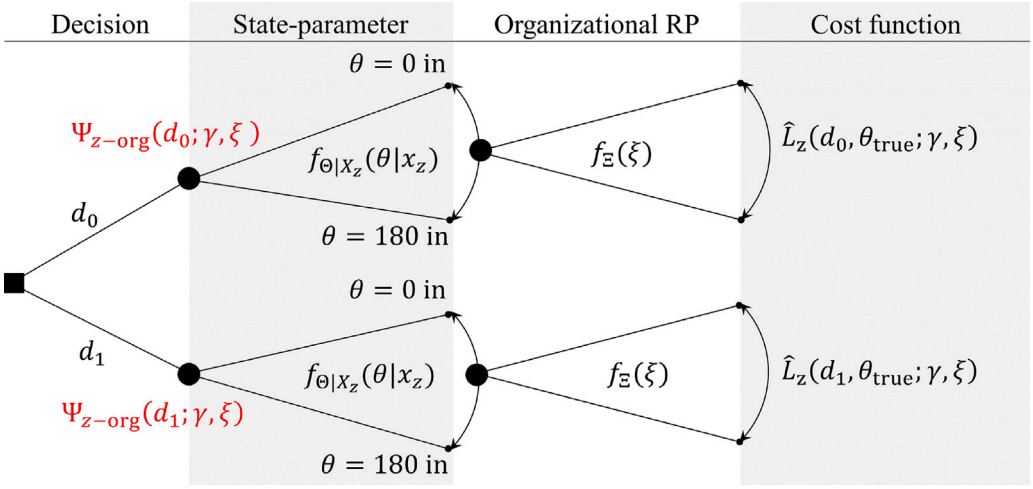

Fig. 10. Decision tree for posterior analysis considering organizational risk profile.

the true value of gap length θ_{true} used for these simulations. This allows us to predict the state of the structure using the classifier threshold $\tilde{\theta}$ as defined in Eq. (27). We observe that our predictions obtained by minimizing the Bayes conditional risk using Eq. (30) are exactly in line with the predictions made using the classifier defined in Eq. (27) (see Table 7), implying that the presented approach is robust. If θ_{true} is not available, then it can be estimated by the mean of the probability distribution of gap length. The predictions obtained from the prior analysis with mean $\mu_\theta = 90$ inches are closer to that of case 3. This is because the posterior distribution for case 3 falls in the middle of the domain Ω_Θ, and as the prior analysis, is almost symmetric about the center of the domain Ω_Θ. This leads the prior distribution and the posterior distribution case 3 to have close values of their mean. However, since no new information was available for the prior analysis, decisions aligning with posterior decision analysis for case 3 clearly show that the results are not useful and indicate that installing an SHM system adds to the value of decision-making. In fact, making a decision using a uniform prior distribution is a matter of uninformed speculation or simply guessing.

Finally, we investigate the impact of organizational risk profile (ORP) on decision-making. We recall our discussion in Section 4.3 on ORP. We assume $\gamma = 0.8$ and $\Omega_\Xi = [0.55, 0.975]$. We define the Bayes risk and optimal decision considering the ORP for prior analysis as:

$$\begin{aligned}
\Psi_{\text{prior-org}}(d_0) &= E_{\Theta\Xi}\left[\hat{L}(d_0, \theta_{\text{true}} = \theta; \gamma, \xi)\right] \\
&= E_{\Theta}\left[E_{\Xi}\left[\hat{L}(d_0, \theta_{\text{true}} = \theta; \gamma, \xi)\right]\right]; \\
\Psi_{\text{prior-org}}(d_1) &= E_{\Theta\Xi}\left[\hat{L}(d_1, \theta_{\text{true}} = \theta; \gamma, \xi)\right] \\
&= E_{\Theta}\left[E_{\Xi}\left[\hat{L}(d_1, \theta_{\text{true}} = \theta; \gamma, \xi)\right]\right]; \\
\mathscr{A}_{\text{prior-org}} &= \underset{d_i}{\text{argmin}}\left(\Psi_{\text{prior-org}}(d_i)\right).
\end{aligned} \tag{31}$$

In the equation above, it is reasonably assumed that the random variables Θ and Ξ are statistically independent. This is a logical assumption because the organizational behavioral risk profile is independent of the state of the structure. Along similar lines, the Bayes risk and optimal decision considering the ORP for posterior analysis are defined as

$$\begin{aligned}
\Psi_{z\text{-org}}(d_0) &= E_{\Theta|X_z}\left[E_{\Xi}\left[\hat{L}_z(d_0, \theta_{\text{true}} = \theta; \gamma, \xi)\right]\right]; \\
\Psi_{z\text{-org}}(d_1) &= E_{\Theta|X_z}\left[E_{\Xi}\left[\hat{L}_z(d_1, \theta_{\text{true}} = \theta; \gamma, \xi)\right]\right]; \\
\mathscr{A}_{z\text{-org}} &= \underset{d_i}{\text{argmin}}\left(\Psi_{z\text{-org}}(d_i)\right).
\end{aligned} \tag{32}$$

Fig. 10 illustrates the decision tree associated with the posterior decision analysis defined in Eq. (32).

For demonstration purposes, we perform posterior decision analysis based on the posterior probability distribution of the gap length shown in Fig. 9 considering the risk profiles ORP1 and ORP2 portrayed in Figs. 5(a) and 5(b), respectively. Table 8 reports the results obtained using posterior decision analysis considering the organizational risk

Table 8
Posterior decision analysis considering organizational risk profiles ORP1 and ORP2.

Cases	ORP1			ORP2		
	$\Psi_{z\text{-org}}(d_0)$	$\Psi_{z\text{-org}}(d_1)$	$\mathscr{d}_{z\text{-org}}$	$\Psi_{z\text{-org}}(d_0)$	$\Psi_{z\text{-org}}(d_1)$	$\mathscr{d}_{z\text{-org}}$
1	0.196	0.216	d_0	0.0905	0.207	d_0
2	0.489	0.258	d_1	0.226	0.230	d_0
3	0.770	0.328	d_1	0.462	0.277	d_1
4	0.930	0.385	d_1	0.703	0.333	d_1
5	0.988	0.409	d_1	0.838	0.372	d_1

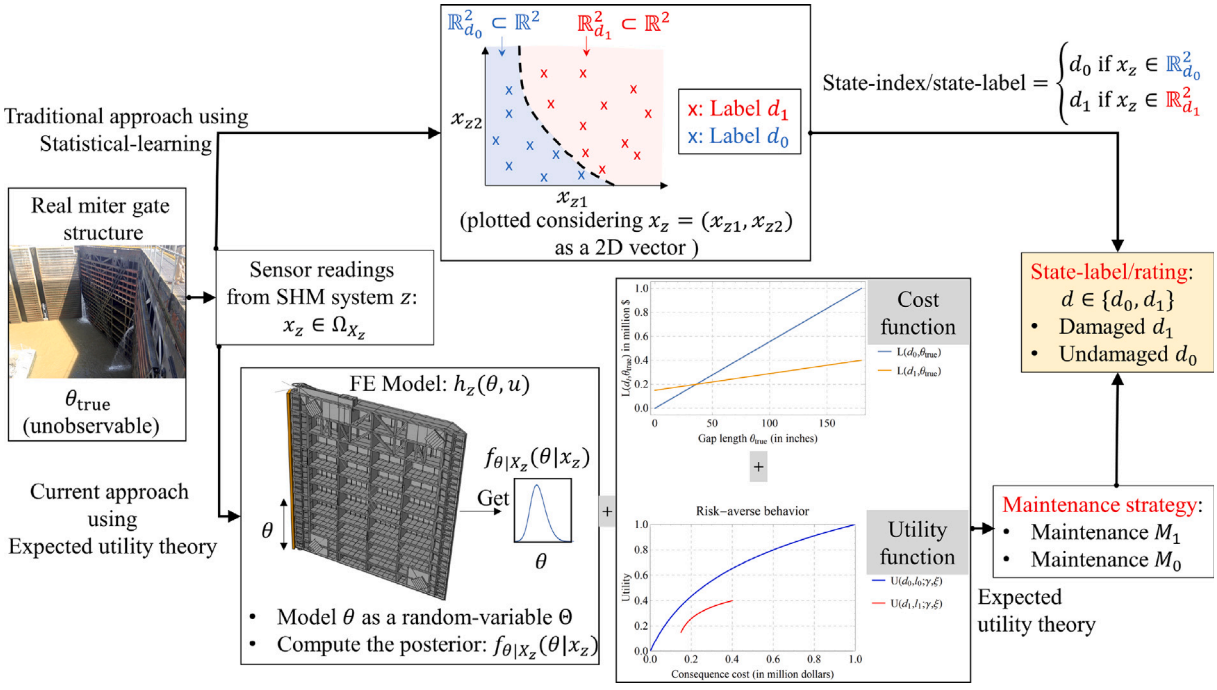

Fig. 11. General methodology.

profiles. As mentioned at the end of Section 4.3, ORP1 is more risk-averse than ORP2. On average, the ORP1 tends to conclude that the gate is damaged at a smaller gap length than the ORP2.

Fig. 11 illustrates our current approach that aims at choosing optimal maintenance actions on an economic basis that minimizes the cost/regret of making decisions while accounting for all sources of uncertainties. This also allows us to rate/classify label the state of the structure because the maintenance strategy is designed, and its consequence-cost evaluated based on a discrete set of damaged ratings. This state-classification approach is different from the traditional machine learning-based detection problem and is more suitable for SHM-related problems. This is because more often than not, these discrete damaged states are hard to define in a meaningful or physical way. Secondly, even if the discrete damaged states are defined, statistical learning requires a large amount of data relating the damaged states to the sensor measurements. This again is challenging – if not impossible – to obtain.

Remark 4. A significant part of the proposed formulation is based on the knowledge of the costs caused by structural failure, loss of life and property, and the cost of replacement, denoted by $\alpha_{\max}$. For the discussion so far, we have assumed that $\alpha_{\max}$ is accurately estimated and known. However, when the failure of an asset involves loss of property and lives (the consequence of which could be determined by the insurance payout), it may be extremely difficult to obtain an accurate value of $\alpha_{\max}$ and it is reasonable to estimate a range of $\alpha_{\max}$. We can include the uncertainty in $\alpha_{\max}$ into the decision-making framework. Let $f_{A_{\max}}(\alpha_{\max})$ denote the probability distribution of the total cost of failure of structure, and loss of life and property, where $A_{\max}$ denotes the random variable with a realization $\alpha_{\max}$. Let $\hat{L}(d_i, \theta_{\text{true}}; \alpha_{\max}, \gamma, \xi)$ denote the consequence curve which in this case is also a function of $\alpha_{\max}$. The optimal decision for the prior and the posterior case is then obtained as:

$$\mathscr{d}_{\text{prior}}(\gamma, \xi) = \underset{d_i}{\operatorname{argmin}}\, E_{\Theta}\left[E_{A_{\max}}\left[\hat{L}\left(d_i, \theta; \alpha_{\max}, \gamma, \xi\right)\right]\right];$$
$$\mathscr{d}_{z}(\gamma, \xi) = \underset{d_i}{\operatorname{argmin}}\, E_{\Theta|X_z}\left[E_{A_{\max}}\left[\hat{L}_z\left(d_i, \theta; \alpha_{\max}, \gamma, \xi\right)\right]\right]. \tag{33}$$

Remark 5. The proposed framework is focused on developing the maintenance policy for a miter gate structure, the health of which is defined by a scalar continuous damage parameter (the gap length). Developing any decision-making policy requires a case-by-case investigation of the problem at hand and is bounded by the complexity and governing physics of the system, the target of the decision-making policy, its alignment with the organizational values, and numerous assumptions made to simplify the decision-making process. For instance, in the context of structural engineering applications, unlike the scalar state parameter used in this paper, the state parameter can be a multidimensional quantity containing numerous engineering demand parameters (EDPs) associated with more than one potential damage/failure mode of a structural system. It is beyond the scope of this paper to tackle such problems; however, in theory, the principles can be extended to such problems. For instance, a multi-dimensional state parameter would require a multi-dimensional consequence cost hypersurface. Specific constraints must be imposed to establish the correlation between various EDPs. The statistical correlations between various EDPs would be a by-product of the propagation of uncertainties through the model of the structure.

6. Conclusion

This paper proposes an approach to determine an optimal maintenance strategy and rate/label the structural-state taking into account the individual or organizational risk profile of the decision-makers. There are consequences associated with making a maintenance decision. In this paper, we consider the consequence costs of performing maintenance actions depending on what the true degree of structural damage (or true state parameter) is. For a particular maintenance strategy (with a unique label), the relationship of the cost-consequence to all the possible values of the true degree of damage (or the state-parameter) is defined by the *consequence cost function*. The consequence cost function is derived for each maintenance strategy by estimating various costs associated with maintenance downtime, inspection, repair or replacement, and the cost of losing lives and property in case of catastrophic failure. It is also assumed that state-parameter completely describes the degree of structural damage. Since the state parameter is assumed to be not directly measurable, it is probabilistically inferred from acquired sensor data (in this paper simulated using the FEM) using Bayesian inference. Among the available predefined set of maintenance strategies, an optimal maintenance strategy is one that minimizes the expected value of the consequence costs. The consequence cost associated with each maintenance label is implicitly designed by considering a true level of damage, thus, choosing an optimal maintenance strategy allows the engineer to reasonably use the associated labels as the state classifier.

The base cost functions are defined by the organization. In most cases, these costs are estimated based on the available data and are approximate. When it comes to maintenance decisions, guided by the organization's maintenance policies, engineers are tasked to decide how to perform the maintenance. These decisions are subjective to the engineer's experience and their thought-process, and risk behavior. Therefore, the maintenance decisions made onsite by the engineers, although as per the organization's recommendations, can have a different cost-consequence as defined by the base cost function. We model these deviations using risk-profile. The risk profile of the decision-maker can be mathematically modeled by their utility vs. wealth (or loss) function or simply *utility function*. An individual's utility gives their evaluation of the consequence/outcome of an action. The utility may be different from the real dollar cost (or value). The base cost function and the utility function can be combined to incorporate the effect of human psychology and an individual's risk-perception into the decision-making model. An organization consists of many decision-makers with a spectrum of risk profiles. Apart from investigating the effect of an individual's risk perception, the collective risk behavior of the organization is also investigated. Finally, the decision analysis is performed using the expected utility theory. The application of the proposed framework to the maintenance of a miter gate validates and demonstrates the applicability of the proposed framework and parametrically analyzes the sensitivity of the optimum decision based on the risk profiles of the decision-maker.

CRediT authorship contribution statement

Mayank Chadha: Conceptualization, Methodology, Formal analysis, Writing – original draft, Writing – review & editing,. **Mukesh K. Ramancha:** Formal analysis, Investigation, Validation, Writing – review & editing. **Manuel A. Vega:** Methodology, Writing – review & editing. **Joel P. Conte:** Methodology, Supervision, Writing – review & editing. **Michael D. Todd:** Conceptualization, Funding acquisition, Project administration, Supervision, Writing – review & editing.

Declaration of competing interest

The authors declare that they have no known competing financial interests or personal relationships that could have appeared to influence the work reported in this paper.

Data availability

Data will be made available on request.

Acknowledgments

Funding for this work was provided by the United States Army Corps of Engineers through the U.S. Army Engineer Research and Development Center Research Cooperative Agreement W912HZ-17-2-0024. Approved for release: LA-UR-21-28992.

References

[1] Farrar CR, Worden K. Structural health monitoring: A machine learning perspective. John Wiley & Sons; 2012.
[2] Farrar C, Park G, Farinholt K, Todd M. Integrated solutions to SHM problems: An overview of SHM research at the LANL/UCSD engineering institute. Tech. rep., Los Alamos National Lab.(LANL), Los Alamos, NM (United States); 2010.
[3] Foltz SD. Investigation of mechanical breakdowns leading to lock closures. Tech. rep., ERDC-CERL CHAMPAIGN United States; 2017.
[4] Vega MA, Hu Z, Todd MD. Optimal maintenance decisions for deteriorating quoin blocks in miter gates subject to uncertainty in the condition rating protocol. Reliab Eng Syst Saf 2020;204:107147.
[5] Barker K, Haimes YY. Assessing uncertainty in extreme events: Applications to risk-based decision making in interdependent infrastructure sectors. Reliab Eng Syst Saf 2009;94(4):819–29.
[6] Lam JYJ, Banjevic D. A myopic policy for optimal inspection scheduling for condition based maintenance. Reliab Eng Syst Saf 2015;144:1–11.
[7] Gomes WJ, Beck AT, Haukaas T. Optimal inspection planning for onshore pipelines subject to external corrosion. Reliab Eng Syst Saf 2013;118:18–27.
[8] Hoseyni SM, Di Maio F, Zio E. Condition-based probabilistic safety assessment for maintenance decision making regarding a nuclear power plant steam generator undergoing multiple degradation mechanisms. Reliab Eng Syst Saf 2019;191:106583.
[9] Phan HC, Dhar AS, Hu G, Sadiq R. Managing water main breaks in distribution networks—-A risk-based decision making. Reliab Eng Syst Saf 2019;191:106581.
[10] Huynh KT, Grall A, Bérenguer C. Assessment of diagnostic and prognostic condition indices for efficient and robust maintenance decision-making of systems subject to stress corrosion cracking. Reliab Eng Syst Saf 2017;159:237–54.
[11] Chen TY-J, Riley CT, Van Hentenryck P, Guikema SD. Optimizing inspection routes in pipeline networks. Reliab Eng Syst Saf 2020;195:106700.
[12] Ito K, Mizutani S, Nakagawa T. Optimal inspection models with minimal repair. Reliab Eng Syst Saf 2020;201:106946.
[13] Yeter B, Garbatov Y, Soares CG. Risk-based maintenance planning of offshore wind turbine farms. Reliab Eng Syst Saf 2020;202:107062.
[14] Bressi S, Santos J, Losa M. Optimization of maintenance strategies for railway track-bed considering probabilistic degradation models and different reliability levels. Reliab Eng Syst Saf 2021;207:107359.
[15] Theissler A, Pérez-Velázquez J, Kettelgerdes M, Elger G. Predictive maintenance enabled by machine learning: Use cases and challenges in the automotive industry. Reliab Eng Syst Saf 2021;215:107864.
[16] Huynh KT. An adaptive predictive maintenance model for repairable deteriorating systems using inverse Gaussian degradation process. Reliab Eng Syst Saf 2021;213:107695.
[17] Thelen A, Zhang X, Fink O, Lu Y, Ghosh S, Youn BD, et al. A comprehensive review of digital twin–Part 1: Modeling and twinning enabling technologies. 2022, arXiv preprint arXiv:2208.14197.
[18] Thelen A, Zhang X, Fink O, Lu Y, Ghosh S, Youn BD, et al. A comprehensive review of digital twin–Part 2: Roles of uncertainty quantification and optimization, a battery digital twin, and perspectives. 2022, arXiv preprint arXiv:2208.12904.
[19] Shi Y, Zhu W, Xiang Y, Feng Q. Condition-based maintenance optimization for multi-component systems subject to a system reliability requirement. Reliab Eng Syst Saf 2020;202:107042.
[20] Zhang F, Shen J, Ma Y. Optimal maintenance policy considering imperfect repairs and non-constant probabilities of inspection errors. Reliab Eng Syst Saf 2020;193:106615.
[21] Shahraki AF, Yadav OP, Vogiatzis C. Selective maintenance optimization for multi-state systems considering stochastically dependent components and stochastic imperfect maintenance actions. Reliab Eng Syst Saf 2020;196:106738.
[22] Hashemi M, Asadi M, Zarezadeh S. Optimal maintenance policies for coherent systems with multi-type components. Reliab Eng Syst Saf 2020;195:106674.
[23] Vu HC, Do P, Fouladirad M, Grall A. Dynamic opportunistic maintenance planning for multi-component redundant systems with various types of opportunities. Reliab Eng Syst Saf 2020;198:106854.
[24] Zhang M. A heuristic policy for maintaining multiple multi-state systems. Reliab Eng Syst Saf 2020;203:107081.
[25] Levitin G, Finkelstein M, Xiang Y. Optimal inspections and mission abort policies for multistate systems. Reliab Eng Syst Saf 2021;214:107700.

[26] Petchrompo S, Li H, Erguido A, Riches C, Parlikad AK. A value-based approach to optimizing long-term maintenance plans for a multi-asset k-out-of-n system. Reliab Eng Syst Saf 2020;200:106924.
[27] Hamdan K, Tavangar M, Asadi M. Optimal preventive maintenance for repairable weighted k-out-of-n systems. Reliab Eng Syst Saf 2021;205:107267.
[28] Fauriat W, Zio E. Optimization of an aperiodic sequential inspection and condition-based maintenance policy driven by value of information. Reliab Eng Syst Saf 2020;204:107133.
[29] Lin C, Song J, Pozzi M. Optimal inspection of binary systems via value of information analysis. Reliab Eng Syst Saf 2022;217:107944.
[30] Vega MA, Hu Z, Yang Y, Chadha M, Todd MD. Diagnosis, prognosis, and maintenance decision making for civil infrastructure: Bayesian data analytics and machine learning. In: Structural health monitoring based on data science techniques. Springer; 2022, p. 45–73.
[31] Yang Y, Chadha M, Hu Z, Vega MA, Parno MD, Todd MD. A probabilistic optimal sensor design approach for structural health monitoring using risk-weighted f-divergence. Mech Syst Signal Process 2021;161:107920.
[32] Yang Y, Chadha M, Hu Z, Todd MD. An optimal sensor placement design framework for structural health monitoring using Bayes risk. Mech Syst Signal Process 2022;168:108618.
[33] Von Neumann J, Morgenstern O, Kuhn HW. Theory of games and economic behavior. Commemorative ed.. Princeton University Press; 2007.
[34] Parmigiani G, Inoue L. Decision theory: Principles and approaches, vol. 812. John Wiley & Sons; 2009.
[35] Bayes T. LII. An essay towards solving a problem in the doctrine of chances. By the late Rev. Mr. Bayes, FRS communicated by Mr. Price, in a letter to John Canton, AMFR S. Philos Trans R Soc Lond 1763;(53):370–418.
[36] Tversky A, Kahneman D. Judgment under uncertainty: Heuristics and biases. Science 1974;185(4157):1124–31.
[37] Thekdi SA, Aven T. A methodology to evaluate risk for supporting decisions involving alignment with organizational values. Reliab Eng Syst Saf 2018;172:84–93.
[38] Hopkins A. Was three mile island a 'normal accident'? J Contingencies Crisis Manag 2001;9(2):65–72.
[39] Buchanan L, O. Connell A. A brief history of decision making. Harv Bus Rev 2006;84(1):32.
[40] Bernoulli D. Exposition of a new theory on the measurement of risk. In: The Kelly capital growth investment criterion: Theory and practice. World Scientific; 2011, p. 11–24.
[41] Plous S. The psychology of judgment and decision making. Mcgraw-Hill Book Company; 1993.
[42] Tversky A, Kahneman D. Prospect theory: An analysis of decision under risk. Econometrica 1979;47(2):263–91.
[43] Tversky A, Kahneman D. Advances in prospect theory: Cumulative representation of uncertainty. J Risk Uncertain 1992;5(4):297–323.
[44] Gardoni P, Guevara-Lopez F, Contento A. The life profitability method (LPM): A financial approach to engineering decisions. Struct Saf 2016;63:11–20.
[45] Tyrrell Rockafellar R, Royset JO. Engineering decisions under risk averseness. ASCE-ASME J Risk Uncertain Eng Syst A 2015;1(2):04015003.
[46] Kroon IB, Hoej NP. Application of risk aversion for engineering decision making. 2001, Safety, Risk and Reliabilitytrends in Engineering, Malta.
[47] Straub D, Faber MH. Risk based inspection planning for structural systems. Struct Saf 2005;27(4):335–55.
[48] Faber MH. On the treatment of uncertainties and probabilities in engineering decision analysis. J Offshore Mech Arct Eng 2005;127(3):243–8.
[49] Faber M, Maes M, Huyse L. Modeling of risk perception in engineering decision analysis. In: Proc IFIP WG, vol. 7. 2004, p. 113–22.
[50] Chadha M, Hu Z, Todd MD. An alternative quantification of the value of information in structural health monitoring. Struct Health Monit 2022;21(1):138–64.
[51] Thöns S. On the value of monitoring information for the structural integrity and risk management. Comput-Aided Civ Infrastruct Eng 2018;33(1):79–94.
[52] Straub D. Value of information analysis with structural reliability methods. Struct Saf 2014;49:75–85.
[53] Zonta D, Glisic B, Adriaenssens S. Value of information: Impact of monitoring on decision-making. Struct Control Health Monit 2014;21(7):1043–56.
[54] Limongelli MP, Omenzetter P, Yazgan U, Soyoz S. Quantifying the value of monitoring for post-earthquake emergency management of bridges. In: Proceedings of 39th IABSE symposium–engineering the future. 2017.
[55] Raiffa H, Schlaifer R. Applied statistical decision theory. Wiley Cambridge; 1961.
[56] Bolognani D, Verzobio A, Tonelli D, Cappello C, Glisic B, Zonta D. An application of prospect theory to a SHM-based decision problem. In: Health monitoring of structural and biological systems 2017, vol. 10170. International Society for Optics and Photonics; 2017, p. 101702G.
[57] Benjamin JR, Cornell CA. Probability, statistics, and decision for civil engineers. Dover Publication; 2014.
[58] Daniel RA. Miter gates in some recent lock projects in the Netherlands (Stemmtore in einigen neuen Schleusenanlagen in den Niederlanden). Stahlbau 2000;69(12):952–64.
[59] Richardson GC. Navigation locks: Navigation lock gates and valves. J Waterw. Harb. Div. 1964;90(1):79–102.
[60] Parno M, O'Connor D, Smith M. High dimensional inference for the structural health monitoring of lock gates. 2018, arXiv preprint arXiv:1812.05529.
[61] Schwieterman JP, Field S, Fischer L, Pizzano A. An analysis of the economic effects of terminating operations at the chicago river controlling works and O'Brien locks on the Chicago area waterway system. 2010, DePaul University, Chicago, IL.
[62] Eick BA, Treece ZR, Spencer Jr. BF, Smith MD, Sweeney SC, Alexander QG, et al. Automated damage detection in miter gates of navigation locks. Struct Control Health Monit 2018;25(1):e2053.
[63] Vega MA, Todd MD. A variational Bayesian neural network for structural health monitoring and cost-informed decision-making in miter gates. Struct Health Monit 2020.
[64] Ramancha M, Astroza R, Conte JP, Restrepo JI, Todd MD. Bayesian nonlinear finite element model updating of a full-scale bridge-column using sequential Monte Carlo. In: Proceedings of the 38th IMAC, a conference and exposition on structural dynamics 2020. Springer; 2021.
[65] Eick BA, Smith MD, Fillmore TB. Feasibility of retrofitting existing miter-type lock gates with discontinuous contact blocks. J Struct Integr Maintenance 2019;4(4):179–94.
[66] Vega MA, Ramancha M, Todd MD, Conte JP. Efficient Bayesian inference of iter gates using high-fidelity models. In: Proceedings of the 38th IMAC, a conference and exposition on structural dynamics 2020. Springer; 2021.
[67] Ramancha MK, Astroza R, Madarshahian R, Conte JP. Bayesian updating and identifiability assessment of nonlinear finite element models. Mech Syst Signal Process 2022;167:108517.
[68] Ramancha MK, Conte JP, Parno MD. Accounting for model form uncertainty in Bayesian calibration of linear dynamic systems. Mech Syst Signal Process 2022;171:108871.
[69] Ching J, Chen Y-C. Transitional Markov chain Monte Carlo method for Bayesian model updating, model class selection, and model averaging. J Eng Mech 2007;133(7):816–32.
[70] Tversky A. Elimination by aspects: A theory of choice. Psychol Rev 1972;79(4):281.
[71] Markowitz H. The utility of wealth. J Polit Econ 1952;60(2):151–8.
[72] Lemaitre J. A course on damage mechanics. Springer Science & Business Media; 2012.
[73] Krauthammer C. The point of it all: A lifetime of great loves and endeavors. Crown Forum; 2018.
[74] Kenneth J. Arrow. Essays in the theory of risk-bearing. North Holland; 1971.
[75] Bernstein PL, Bernstein PL. Against the gods: The remarkable story of risk. Wiley New York; 1996.
[76] Pratt JW. Risk aversion in the small and in the large. In: Uncertainty in economics. Elsevier; 1978, p. 59–79.
[77] Soros G. The alchemy of finance. John Wiley & Sons; 2015.